Effects of Relative Permeability on Parameter Estimation

A REPORT
SUBMITTED TO THE DEPARTMENT OF PETROLEUM ENGINEERING
OF STANFORD UNIVERSITY
IN PARTIAL FULFILLMENT OF THE REQUERIMENTS
FOR THE DEGREE
OF MASTER OF SCIENCE

By

Martin Javier Cocco

August 2002

I certify that I have read this report and that in my opinion it is fully adequate, in scope and in quality, as partial fulfillment of the degree of Master of Science in Petroleum Engineering.

Dr. Roland N. Horne
(Principal Advisor)

Abstract

A new approach to determine the influence of the relative permeabilities in the parameter estimation problem is presented in this work. Relative permeabilities govern the multiphase flow; therefore, they have a significant importance in understanding the reservoir behavior. Traditionally, relative permeabilities have been assumed as known parameters when the inverse problem is solved. This assumption introduces a new source of uncertainty in the reservoir model. The aim of this work was to study the influence of the relative permeability when automatic history matching is performed to determine reservoir parameters such as porosities and absolute permeabilities. In this work, relative permeabilities were parameterized using Corey type curves and including them into the inverse model as six additional parameters. The results obtained show the impact that using wrong relative permeabilities has on the estimated parameters. Finally, several suggestions to minimize the uncertainty introduced by the relative permeabilities are made.

Acknowledgements

First and foremost, I would like to thank my advisor, Dr. Roland N. Horne, for the support and patience he has given me during the course of this project providing me invaluable advice and assistance in my research.

I am grateful for the generous financial support of my graduate studies provided by Stanford University Petroleum Research Institute (SUPRI-D) and the Department of Petroleum Engineering of Stanford University.

Gratitude is expressed to Vinh Phan who supplied me with the base computer code used in this work.

My Special thanks to Andres for his invaluable suggestions and encouragements helping me to overcome those difficult moments during my research and my life at Stanford.

Also, special thanks to Melissa for her outstanding support and for being so *chevere* with me.

Thanks to all the friends that made my life at Stanford so pleasant, Xyoli, Manuel, Sandra, Oscar and Rita.

Finally, tons of thanks to my Dad and Mom and my brother Facundo for their encouragement and everlasting love.

Contents

Abstract v

Acknowledgments vi

Table of Contents ix

List of Tables xi

List of Figures xii

1 Introduction 1

2 Mathematical Background 3

2.1 Forward Problem Equations 5

2.2 Objective Function 9

2.3 Objective Function Minimization 9

2.4 Sensitivity Coefficients 13

3 Results and Discussion 17

Reservoir

3.1 Model 17

3.2 Sensitivity Coefficients Analysis 18

3.3 Influence of Relative Permeabilities on Estimated Absolute Permeabilities 18

3.4 Influence of Relative Permeabilities on Estimated Porosities 19

4 Conclusions and Recommendations …… 51

Nomenclature ……... 53

Bibliography ……...….. 57

List of Tables

3.1 Reservoir properties …..... 21

3.2 Relative permeability parameters 22

List of Figures

2.1 Forward problem ….…..…….…. 3

2.2 Inverse problem ….....…….…. 4

2.3 Inverse problem general algorithm 4

3.1 Reservoir grid ….....…….…. 21

3.2 Relative permeability curves ….....…….…. 22

3.3 Bottom hole pressure for injector and producer wells 23

3.4 Water cut for injector and producer wells …….. 23

3.5 Flow rate for producer well .....….....…….…. 24

3.6 Flow rate for injector well .....…….…….…. 24

3.7 Sensitivity of pressure and water cut at producer with respect to the relative permeability parameters 25

3.8 Match of bottom hole pressure and water cut for absolute permeabilities (*x*-coordinate) and the end point of the water relative permeability ….…….. 26

3.9 Estimated absolute permeabilities (*x*-coordinate) and the end point of the water relative permeability curve .....…….....….....…….…. 27

3.10 Match of bottom hole pressure and water cut for absolute permeabilities (*x*-coordinate) and the exponent of the water relative permeability curve…….…….…….….. 28

3.11 Estimated absolute permeabilities (*x*-coordinate) and the exponent of the water relative permeability curve 29
3.12 Match of bottom hole pressure and water cut for absolute permeabilities (*x*-coordinate) and connate water saturation 30
3.13 Estimated absolute permeabilities (*x*-coordinate) and connate water saturation ... 31
3.14 Match of bottom hole pressure and water cut for absolute permeabilities (*x*-coordinate) and the end point of the oil relative permeability curve 32
3.15 Estimated absolute permeabilities (*x*-coordinate) and the end point of the oil relative permeability curve..... 33
3.16 Match of bottom hole pressure and water cut for absolute permeabilities (*x*-coordinate) and the exponent of the oil relative permeability curve..... 34
3.17 Estimated absolute permeabilities (*x*-coordinate) and the exponent of the oil relative permeability curve..... 35
3.18 Match of bottom hole pressure and water cut for absolute permeabilities (*x*-coordinate) and residual oil saturation..... 36
3.19 Estimated absolute permeabilities (*x*-coordinate) and oil residual saturation..... 37
3.20 Match of bottom hole pressure and water cut for porosities and the end point of the water relative permeability curve..... 38
3.21 Estimated porosities and the end point of the water relative permeability curve..... 39
3.22 Match of bottom hole pressure and water cut for porosities (*x*-coordinate) and the exponent of the water relative permeability curve..... 40
3.23 Estimated porosities and the exponent of the water relative permeability curve..... 41
3.24 Match of bottom hole pressure and water cut for porosities and connate water saturation..... 42
3.25 Estimated porosities and connate water saturation..... 43
3.26 Match of bottom hole pressure and water cut for porosities and the end point of the oil relative permeability curve..... 44

3.27 Estimated porosities and the end point of the oil relative permeability curve…….....…..…..…..…..…..…..…….....…..…..…..…..…….…….... 45

3.28 Match of bottom hole pressure and water cut porosities and the exponent of the oil relative permeability curve…….…… 46

3.29 Estimated porosities and the exponent of the oil relative permeability curve…..... 47

3.30 Match of bottom hole pressure and water cut for porosities and residual oil saturation…….…..……...…..…..…..…..…..……..... 48

3.31 Estimated porosities and oil residual saturation……..…… 49

Section 1

Introduction

In the modern petroleum industry, automated history matching using mathematical reservoir models plays a useful role in order to estimate reservoir parameters such as porosity and absolute permeability. These parameters are then used to develop reservoir performance predictions, economic estimations, infill well placement and many other decisions during the reservoir life. However, the accuracy of the reservoir predictions depends not only on the reservoir mathematical and numerical models but also on the quality of the data supplied. One of the most important parameters in reservoir property estimation is relative permeability since it governs the multiphase flow behavior.

Relative permeabilities can be obtained from different sources. One source is core flooding techniques such as described by Jensen et al. (1959). The main drawback of these experimental determinations arises from the core size because no matter which laboratory technique is used, cores represent a small fraction of the reservoir which normally does not consider large scale heterogeneities. Another source of relative permeabilities are mathematical models. Several correlations have been formulated in order to depict reservoir relative permeabilities such as those proposed by Corey (1954) or Coats (1971). However, correlations are not general and, consequently, they may not be suitable for all reservoirs. Works of Al-Labban (1990) and Mamora (1990) attempted

to overcome these shortcomings by matching production data. However, in their approaches, the rest of the reservoir parameters such as porosities and absolute permeabilities must be known. More recent works in automatic history matching, Landa (1996 and 1997) and Phan (1999 and 2002) integrated several sources of static and dynamic data in more effective computational algorithms in two-dimensional and three-dimensional reservoir models. These models assumed that the relative permeabilities for each phase are known from Corey correlations.

From the mathematical standpoint, because the history matching is an ill-posed problem, introducing inaccurate relative permeability values may cause the solution to diverge or to match the production history but with incorrect parameters. The second scenario is the most significant since it would give a false impression of achieving the right reservoir description.

The aim of this work was to study the influence of the relative permeabilities on the distributed parameter estimation when history matching is performed. The relative permeabilities were parameterized using the Corey model and included in the inverse mode. Thus, the relative permeability parameters were treated as additional unknowns along with porosities and absolute permeabilities.

Section 2

Mathematical Background

The reservoir can be modeled by means of mathematical equations. These equations must be capable of representing or predicting the physical behavior of the reservoir when it is under an external perturbation (e.g. change in well rates). In this case, reservoir parameters (absolute and relative permeabilities and porosities) are known. This situation is called the forward problem and can be schematized as in Figure 2.1.

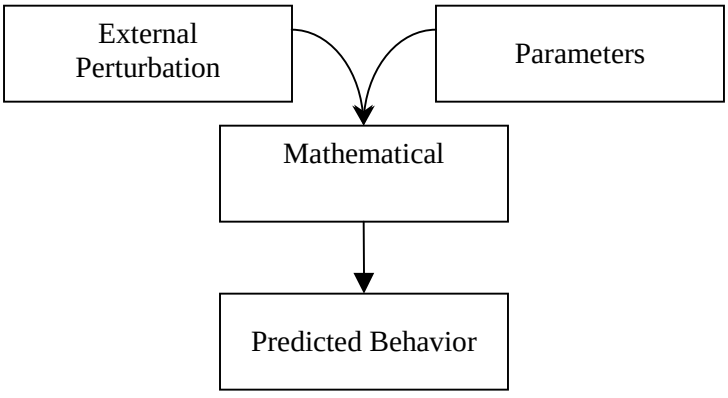

Figure 2.1: Forward problem.

Alternatively, in reservoir characterization problems, the reservoir parameters are unknown. For these cases, the idea is to find a set of parameters that reproduce the true

reservoir behavior when an external perturbation is applied. This second situation is referred to as an inverse problem, as in Figure 2.2.

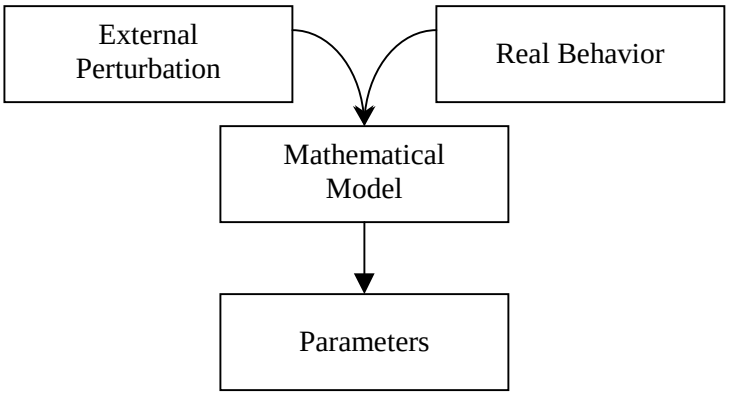

Figure 2.2: Inverse problem.

Defining the inverse problem can be divided into three main sections:

- Mathematical model.
- Objective function.
- Objective function minimization.

The general algorithm used to solve the inverse problem is shown in Figure 2.3.

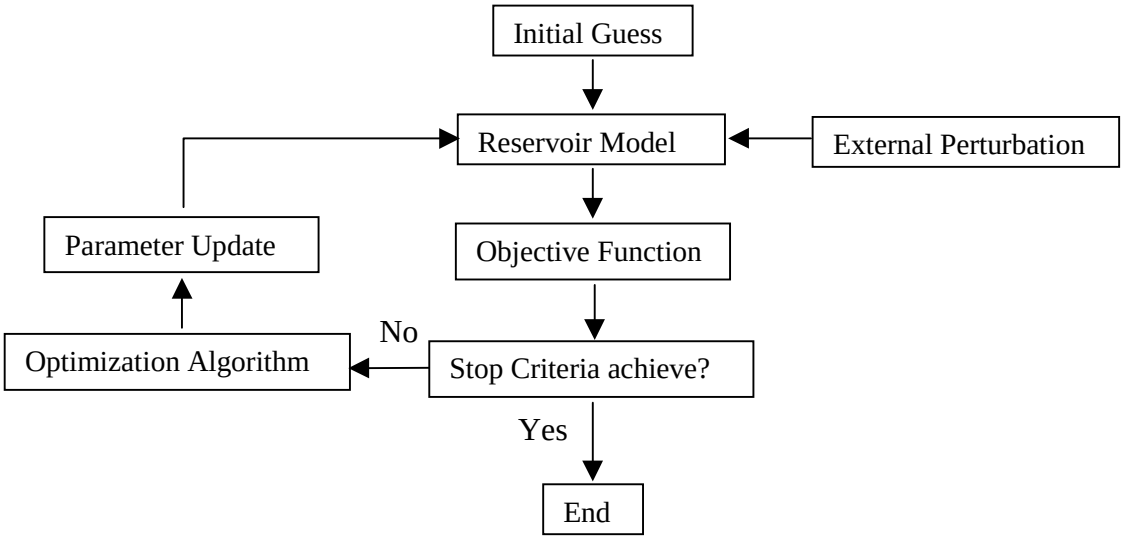

Figure 2.3: Inverse problem general algorithm.

Assuming an initial guess of the parameters, the reservoir model is initialized and the response due to the external perturbation is calculated. The objective function compares the simulated response with the real response. Then, the stopping criteria are checked; if these criteria are not reached, the optimization subroutine is called to generate a new parameter set and the reservoir response is compute again. This loop is repeated until the stopping criteria are reached.

2.1 Forward Problem Equations

In order to solve the forward model, a mathematical system of equations is required. This mathematical system is based on physical laws that govern the reservoir fluid dynamics:

- Law of mass conservation.
- Darcy's law.
- Capillary pressure equations.
- Relative permeability equations.
- Equations of state.

The law of mass conservation is a material balance written for a component in a representative elementary volume of the system modeled. Let V be a representative elementary volume whose surface S is crossed by a flux of mass of component c. Assuming that the mass transfer by dispersion and diffusion is negligible and isothermal and no chemical reaction occurs, the law of mass conservation for reservoir standard conditions can be stated as:

Inflow of *c* across the	-	Outflow of *c* across the	+	Sink/Source term	=	Accumulation of *c* within	(2.1)

Rewriting Equation (2.1) for a system with *np* phases:

$$\sum_{p=1}^{np} \oint_S \frac{R_{c,p}}{B_p} \vec{u}_p \, \vec{n} \, dS - \sum_{p=1}^{np} \int_V \frac{R_{c,p}}{B_p} \tilde{q}_p \, dV = \sum_{p=1}^{np} \int_V \frac{\partial}{\partial t} \left(\phi \frac{R_{c,p}}{B_p} S_p \right) dV \tag{2.2}$$

The surface integral in Equation (2.2) may be change into a volume integral through the divergence theorem. Besides, the representative elementary volume may approach to zero since it is chosen arbitrarily. Thus, Equation (2.2) is written as:

$$\sum_{p=1}^{np} \nabla \cdot \left(\frac{R_{c,p}}{B_p} \vec{u}_p \vec{n} \right) + q_c + \sum_{p=1}^{np} \frac{\partial}{\partial t} \left(\phi \frac{R_{c,p}}{B_p} S_p \right) = 0 \tag{2.3}$$

where q_c is the flow rate of component c per unit reservoir volume at standard conditions such:

$$q_c = \sum_{p=1}^{np} \frac{R_{c,p}}{B_p} \tilde{q}_p \tag{2.4}$$

Equation (2.3) is the material balance differential form for component *c*. For the purpose of this work, two immiscible components are considered, oil and water; consequently, two phases will be present in the reservoir at maximum. Since there is no gas present, both fluids are considered slightly compressible. In addition, capillary forces are neglected. The resulting material balance equations for each phase are:

$$\nabla \cdot \left(\frac{\vec{u_o}}{B_o} \right) + \frac{\partial}{\partial t} \left(\phi \frac{R_o}{B_o} S_o \right) + q_o = 0 \tag{2.5}$$

$$\nabla \cdot \left(\frac{\overrightarrow{u_w}}{B_w} \right) + \frac{\partial}{\partial t} \left(\phi \frac{R_w}{B_w} S_w \right) + q_w = 0 \tag{2.6}$$

Darcy's Law is the equation that governs the motion of the fluid through the porous media and can be written for each phase as follow:

$$\vec{u}_o = -\underline{\underline{k}} \left(\frac{k_{ro}}{\mu_o} \right) (\nabla p_o - \rho_o g \nabla z) \tag{2.7}$$

$$\vec{u}_w = -\underline{\underline{k}} \left(\frac{k_{rw}}{\mu_w} \right) (\nabla p_w - \rho_w g \nabla z) \tag{2.8}$$

For Equations (2.7) and (2.8) it was assumed that the medium is heterogeneous and isotropic and Cartesian coordinates with z-axis vertical and oriented downwards.
Substituting Equations (2.5) and (2.6) into Equations (2.7) and (2.8) respectively the forward model main equations are obtained:

$$\nabla \left(\underline{\underline{\lambda_o}} (\nabla p_o - \rho_o g \nabla z) \right) + q_o = \frac{\partial}{\partial t} \left(\phi \frac{S_o}{B_o} \right) \tag{2.9}$$

$$\nabla \left(\underline{\underline{\lambda_w}} (\nabla p_w - \rho_w g \nabla z) \right) + q_w = \frac{\partial}{\partial t} \left(\phi \frac{S_w}{B_w} \right) \tag{2.10}$$

where λ_o and λ_w are the mobilities for oil and water phases respectively defined as:

$$\lambda_p = \underline{\underline{k}} \left(\frac{k_{r,p}}{B_p \mu_p} \right) \qquad p = o, w \tag{2.11}$$

In order to take into account the variation in the pore volume caused by changes in the pressure gradient, the following approximation is used to calculate the reservoir porosities:

$$\phi = \phi^0 \left(1 + c_R \left(p - p^0\right)\right) \tag{2.12}$$

Additionally, relative permeabilities are parameterized using Corey curves (Corey 1954)

$$k_{ro} = k_{ro}^* \left(\frac{1 - S_w - S_{wc}}{1 - S_{wc} - S_{or}} \right)^{n_o} \tag{2.13}$$

$$k_{rw} = k_{rw}^* \left(\frac{S_w - S_{wc}}{1 - S_{wc} - S_{or}} \right)^{n_w} \tag{2.14}$$

Given the fact that the fluids are assumed slightly compressible, formation volume factors for both oil and water become:

$$\frac{1}{B_o} = \frac{1}{B_o^0} \left(1 + c_o \left(p - p^0\right)\right) \tag{2.15}$$

$$\frac{1}{B_w} = \frac{1}{B_w^0} \left(1 + c_w \left(p - p^0\right)\right) \tag{2.16}$$

Similarly, density equations can be written for oil and water:

$$\rho_o = \rho_o^0 \left(1 + c_o \left(p - p^0\right)\right) \tag{2.17}$$

$$\rho_w = \rho_w^0 \left(1 + c_w \left(p - p^0\right)\right) \tag{2.18}$$

The forward model is isothermal and the viscosities of the oil and water are weak functions of the pressure, so assuming that they are constant will not introduce a great deal of error in the results and will save programming and computational time.

2.2 Objective Function

The main aim of the reservoir parameter estimation problem is to find a set of parameters such that the reservoir mathematical model response is as close as possible to the real reservoir response. In order to measure the agreement and minimize the discrepancy of both responses, an objective function must be constructed. The objective function with most extensive use is the weighted least squares:

$$E = \sum_{i=1}^{nobs} w_i \left(d_i^{obs} - d_i^{calc} \right)^2 \tag{2.19}$$

where *nobs* are the number of observed data and *E*, the error, is a measure of discrepancy between the observed data, d_i^{obs} and the resulting data generated by the mathematical reservoir model d_i^{cac}. The observed data used in this work were the bottom hole pressures and water cuts so weight factors, w_i, must be included into the sum to account for their different order of magnitude.

2.3 Objective Function Minimization

The central requirement is to minimize the objective function means to find a set of parameters, $\vec{\alpha} = \vec{\alpha}^*$, such that:

$$E(\vec{\alpha}^*) = \min_{\vec{\alpha}} E(\vec{\alpha}) \tag{2.20}$$

$$\vec{\alpha} = \begin{bmatrix} \vec{\varphi} \\ \vec{k} \\ \vec{k}_r \end{bmatrix} \tag{2.21}$$

$\vec{\varphi}$ Porosity vector
$\vec{k}$ Absolute permeability vector
$\vec{k}_r$ Relative permeability vector

As previously done by Landa (1997) and Phan (1998 and 2002), this work used the Gauss-Newton algorithm for parameter estimation. In the same fashion as other gradient methods, Gauss-Newton assumes that for a given $\vec{\alpha}_0$ such that $\nabla E \neq 0$, it is always possible to decrease the value of *E* by finding a descent direction and an adequate step size.

$$E(\vec{\alpha}_0) > E(\vec{\alpha}_0 + \delta\ \vec{p}) \tag{2.22}$$

$\vec{p}$ descent direction with $\|\vec{p}\| = 1$
δ step size with $\delta > 0$

For unconstrained minimization, assuming that *E* is a smooth function, the necessary conditions for $\vec{\alpha}^*$ to be a minimum are:

$$\nabla E(\vec{\alpha}^*) = \left.\frac{\partial E}{\partial \vec{\alpha}}\right|_{\vec{\alpha}^*} = 0 \tag{2.23}$$

and

$$\vec{\alpha}^T \underline{\underline{H}}^* \vec{\alpha} > 0 \quad \forall \vec{\alpha} \neq 0 \tag{2.24}$$

where $\underline{\underline{H}}$ is the Hessian matrix of second derivatives of *E*,

$$\underline{\underline{H}} = \frac{\partial \nabla E}{\partial \vec{\alpha}} \tag{2.25}$$

Since *E* is assumed to be smooth, it can be linearized by means of a second-order Taylor expansion in the neighborhood of $\vec{\alpha}_0$:

$$E(\vec{\alpha}) = E(\vec{\alpha}_0 + \Delta\vec{\alpha}) \approx E(\vec{\alpha}_0) + \nabla E^T(\vec{\alpha}_0)\Delta\vec{\alpha} + \frac{1}{2}\Delta\vec{\alpha}^T \underline{\underline{H}}(\vec{\alpha}_0)\Delta\vec{\alpha} \tag{2.26}$$

Calculating the gradient of Equation (2.26) and setting it equal to zero:

$$\underline{\underline{H}}(\vec{\alpha}_0)\Delta\vec{\alpha} = -\nabla E(\vec{\alpha}_0) \tag{2.27}$$

Computing the descent direction using Equation (2.27) is known as Newton's method. Premultiplying Equation (2.27) by $\Delta\vec{\alpha}^T$:

$$\Delta\vec{\alpha}^T \underline{\underline{H}}\, \Delta\vec{\alpha} = -\Delta\vec{\alpha}^T \nabla E \tag{2.28}$$

Newton's method has the significant advantage of fast (quadratic) convergence; however, a descent direction is not guaranteed if the second derivatives in the Hessian matrix is not positive-definite. Another important shortcoming of this method is the fact that the Hessian matrix must be computed, which may be expensive in computation time. The Gauss-Newton method makes use of structure of the objective function structure in order to calculate a positive-definite approximation to the Hessian matrix which only requires

the first derivatives (less expensive to compute) and when closing to the minimum the convergence is still quadratic. Writing Equation (2.19) in matrix notation:

$$E(\vec{\alpha}) = \left(\vec{d}^{\,obs} - \vec{d}^{\,calc}\right)^T \underline{\underline{W}} \left(\vec{d}^{\,obs} - \vec{d}^{\,calc}\right) \tag{2.29}$$

with,

$$\vec{d}^{\,obs} - \vec{d}^{\,calc} = \begin{bmatrix} \vec{p}_{wf}^{\,obs} - \vec{p}_{wf}^{\,calc}(\vec{\alpha}) \\ \vec{w}_{ct}^{\,obs} - \vec{w}_{ct}^{\,calc}(\vec{\alpha}) \end{bmatrix} \tag{2.30}$$

$\underline{\underline{W}}$ Symmetric matrix of constant weight factors
$\vec{p}_{wf}$ Vector of bottom hole pressures
$\vec{w}_{ct}$ Vector of water cut values

and differentiating Equation (2.30) with respect to the parameters,

$$\frac{\partial\left(\vec{d}^{\,obs} - \vec{d}^{\,calc}\right)}{\partial\vec{\alpha}} = -\frac{\partial\vec{d}^{\,calc}}{\partial\vec{\alpha}} \equiv -\underline{\underline{G}} \tag{2.31}$$

Using Equation (2.31) the gradient and the Hessian matrix of *E* can be written as:

$$\nabla E = -2\,\underline{\underline{G}}^T \underline{\underline{W}} \left(\vec{d}^{\,obs} - \vec{d}^{\,calc}\right) \tag{2.323}$$

$$\underline{\underline{H}} = \frac{\partial\nabla E}{\partial\vec{\alpha}} = -2\frac{\partial\left(\underline{\underline{G}}^T \underline{\underline{W}}\left(\vec{d}^{\,obs} - \vec{d}^{\,calc}\right)\right)}{\partial\vec{\alpha}} = 2\underline{\underline{G}}^T \underline{\underline{W}}\,\underline{\underline{G}} - 2\left[\vec{u}_1 \cdots \vec{u}_i \cdots \vec{u}_{npar}\right] \tag{2.33}$$

defining $\vec{u}_i$ as:

$$\vec{u}_i \equiv \frac{\partial\underline{\underline{G}}^T}{\partial\alpha_i}\underline{\underline{W}}\left(\vec{d}^{\,obs} - \vec{d}^{\,calc}\right) \tag{2.34}$$

and the Gauss-Newton Hessian matrix, $\underline{\underline{H}}_{GN}$, is defined from Equation (2.33) as follows:

$$\underline{\underline{H}}_{GN} \equiv 2\underline{\underline{G}}^T \underline{\underline{W}}\,\underline{\underline{G}} \tag{2.35}$$

and Equation (2.27) becomes:

$$\underline{\underline{H}}_{GN}(\vec{\alpha}_0)\Delta\vec{\alpha} = -\nabla E(\vec{\alpha}_0) \tag{2.36}$$

Provided that the weight matrix is positive-definite, the Gauss-Newton Hessian is guaranteed to be at least semipositive-definite. The lack of positive-definiteness arises form the fact that the reservoir parameters have different degree of influence on the reservoir response; thus, columns of the sensitivity matrix, $\underline{\underline{G}}$, may vary several orders of magnitude making the $\underline{\underline{H}}_{GN}$ either singular or ill-conditioned. A common approach to stabilize Gauss-Newton Hessian and overcome the difficulties above mentioned is the modified Cholesky factorization method which introduces increments in the diagonal elements of $\underline{\underline{H}}_{GN}$ producing a positive-definite matrix. A detailed description of this method can be found in Gill, Murray and Wright (1981).

2.4 Sensitivity Coefficients

The objective function, *E*, depends on the model response which is a function of the reservoir parameters as can be seen from Equations (2.29) and (2.30). Hence, computing the derivatives of the objective function means to compute the derivatives of *E* with respect to the model response and then the derivatives of the model response with respect to the parameters. The derivatives of the model response with respect to the parameters are called sensitivity coefficients and are defined as:

$$\nabla d = \left(\frac{\partial \vec{d}}{\partial \vec{\alpha}}\right)^T = \begin{bmatrix} \frac{\partial d(\vec{x},t,\vec{\alpha})}{\partial \alpha_1} \\ \vdots \\ \frac{\partial d(\vec{x},t,\vec{\alpha})}{\partial \alpha_i} \\ \vdots \\ \frac{\partial d(\vec{x},t,\vec{\alpha})}{\partial \alpha_{npar}} \end{bmatrix} \tag{2.37}$$

where

$$\vec{\alpha} = \left(\vec{\varphi}, \vec{k}, \vec{k}_r\right) \tag{2.38}$$

A computationally efficient procedure was one of the central points of the work of Landa (1997) to calculate the sensitivity coefficients respect to porosities and absolute permeabilities. The current work need Landa's approach to compute the sensitivity coefficients with respect to absolute permeability and the less substitution approach to calculate the sensitivity coefficients with respect to the relative permeabilities.
The substitution method can be represented in the following scheme:

1. Set $\vec{\alpha} = \vec{\alpha}_0$
2. Solve $d_0 = d(\vec{x}, t, \vec{\alpha}_0)$
3. For *i*=1 to *npar*
   i) $\vec{\alpha}_i = \vec{\alpha}_{0_i} + \varepsilon_i$ where ε_i are small numbers.
   ii) Solve $d = d(\vec{x}, t, \vec{\alpha})$.
   iii) $\left.\frac{\partial d}{\partial \alpha_i}\right|_{\vec{\alpha}=\vec{\alpha}_0} \approx \frac{d - d_0}{\varepsilon_i}$
4. End.

Including the relative permeabilities to the parameter estimation problem will add only six additional parameters. Despite the fact this method is not so computationally efficient,

the small number of new parameters added will not decrease the overall performance of the estimation algorithm to a great extent. The advantage is a significant gain in algorithm simplicity.

Section 3

Results and Discussion

3.1 Reservoir Test Model

The reservoir test model consisting of a single-layer quarter five-spot configuration, as shown in Figure (3.1), was used in all of the studied cases. The grid consists of 10 x 10 x 1 grid blocks. The length of each grid block in *x* and y directions is 132 ft and 100 ft in the *z* direction. The value of absolute permeability was set to 500 md in *x*, *y* and *z* directions for each grid block. Porosity of all grid blocks is 20% and the rock compressibility is 4.8×10^{-6} $psia^{-1}$ both at reference pressure of 3600 psia. The top of the reservoir is at 8000 ft. Oil and water formation volume factor are 1.0 RB/STB at a reference pressure of 3600 psia. Compressibility for oil and water are 5.6×10^{-6} $psia^{-1}$ and 8.0×10^{-6} $psia^{-1}$ respectively at reference conditions of 14.7 psia. Reference densities for oil and water are 49.1 lb/ft^3 and 64.8 lb/ft^3 respectively at standard conditions. Viscosities are assumed constant and are 5 cp for oil and 0.29 cp for water. The reservoir temperature is assumed constant at 692 °R. A summary of the reservoir model data is shown in Table (3.1). Relative permeability curves are shown in Figure (3.2) and Table (3.2) shown the values used to generate these curves. Data for both wells were generated with the numerical simulator and can be seen in Figures (3.3) through (3.6).

3.2 Sensitivity Coefficients Analysis

Sensitivity coefficients for all relative permeability parameters were calculated for an arbitrary grid block and the results are illustrated in Figure (3.7). Before the waterfront arrival, sensitive coefficients are zero. A peak in sensitive coefficients occurs when the waterfront arrives and then the values decrease (in terms of absolute value) after the waterfront arrival. Since sensitivity coefficients can be interpreted in terms information about the data, from Figure (3.7) it can be said that most of the information about the parameters is contained in the waterfront; therefore, it is important to gather pressure and water cut data when the breakthrough takes place. Besides, Figure (3.7) shows the relation between the parameters. The sensitivity for the exponent n_w has an opposite sign to the other two parameters relative permeability end point and residual saturation. This relation means that an increase in n_w will necessarily produce a decrease in the remaining parameters.

3.3 Influence of Relative Permeabilities on Estimated Absolute Permeabilities

Using the data set generated with the numerical simulator, absolute permeability in the *x*-direction was set as unknown with an initial guess of 300md for all blocks. In addition, relative permeability parameters were set as unknowns one at a time totalizing six cases. Initial guesses for relative permeability parameters and results are summarized in Figures (3.8) through (3.19). In all cases, a good agreement between the production data and the calculated data was achieved except for the case of the connate water saturation, Figure (3.12), where the matching curves present some discrepancies with respect to the original history. In addition, inversions that include matching residual saturations have more difficult convergence and the computational time is higher than for the other cases. This

behavior occurs because to modify residual saturations implies that both relative permeability curves change resulting in a harder matching process. Calculated permeability maps show a great deal of discrepancy compared to the true maps demonstrating that matching the production history will not assure the correctness of the inversion. From the permeability maps, it can be seen that the reservoir permeability distribution follow two different patterns, a central zone of high permeabilities connecting both wells surrounded by two zones of low permeabilities and two external zones of high permeabilities separated by a single central zone of low permeability at the center of the reservoir. However, no matter which pattern is obtained the averages of the calculated permeabilities are close to the true permeability average. This means that some geological information should be supplied in order to constrain the inversion not in terms of local values but in the reservoir big picture avoiding this kind of channel pattern result. Furthermore, including water relative permeability parameters into the inverse problem results in higher absolute permeability averages. Even for those cases where the estimated relative permeability parameters were close to the true values the absolute permeability distribution is not close to the right one.

3.4 Influence of Relative Permeabilities on Estimated Porosities

The same data set generated with the numerical simulator was used in this section. As initial guess for porosity a value of 10 % for all blocks was chose. Initial guesses for relative permeability parameters and results are summarized in Figures (3.20) through (3.31). Except for the connate water saturation case, the calculated history matches the numerical data set. As explained in previous section, including the residual saturations in the inverse problem leads to more difficult convergence and CPU time because both relative permeability curves are modified simultaneously. Regarding the porosity distribution, the results obtained are much better a those obtained for absolute

permeability distribution. The porosity distribution seems to be less sensitive to the relative permeability values than the absolute permeability distribution. Even when the production data could not be matched so precisely, as Figure (3.24) illustrates, the porosity distribution calculated agrees reasonably with the true distribution Figure (3.25). Moreover, the average of the calculated porosities for all cases is equal or almost equal to the true average confirming the low dependence of the porosity distribution on the relative permeability.

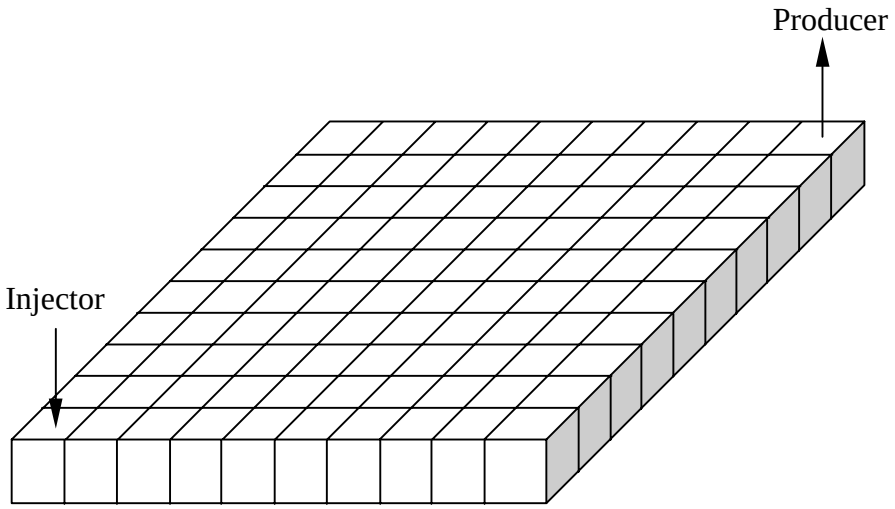

Figure (3.1): Reservoir grid.

$\Delta x = \Delta y$	132 ft
Δz	50 ft
Reservoir Top	8000 ft
k_x	500 md
k_y	500 md
k_z	500 md
ϕ^0	20 % @ 3600 psia
B_o	1 RB/STB
B_w	1 RB/STB
μ_o	5.00 cp
μ_w	0.29 cp
ρ_o	49.1 lb/ft^3 @ 14.7 psia
ρ_w	64.8 lb/ft^3 @ 14.7 psia
C_R	4.8 x 10^{-6} psia^{-1}@ 3600 psia
C_o	8.0 x 10^{-6} psia^{-1} @ 14.7 psia
C_w	5.6 x 10^{-6} psia^{-1} @ 14.7 psia
$T_{reservoir}$	692 ^{o}R
P_{int}	2500 psia

Table (3.1): Reservoir properties

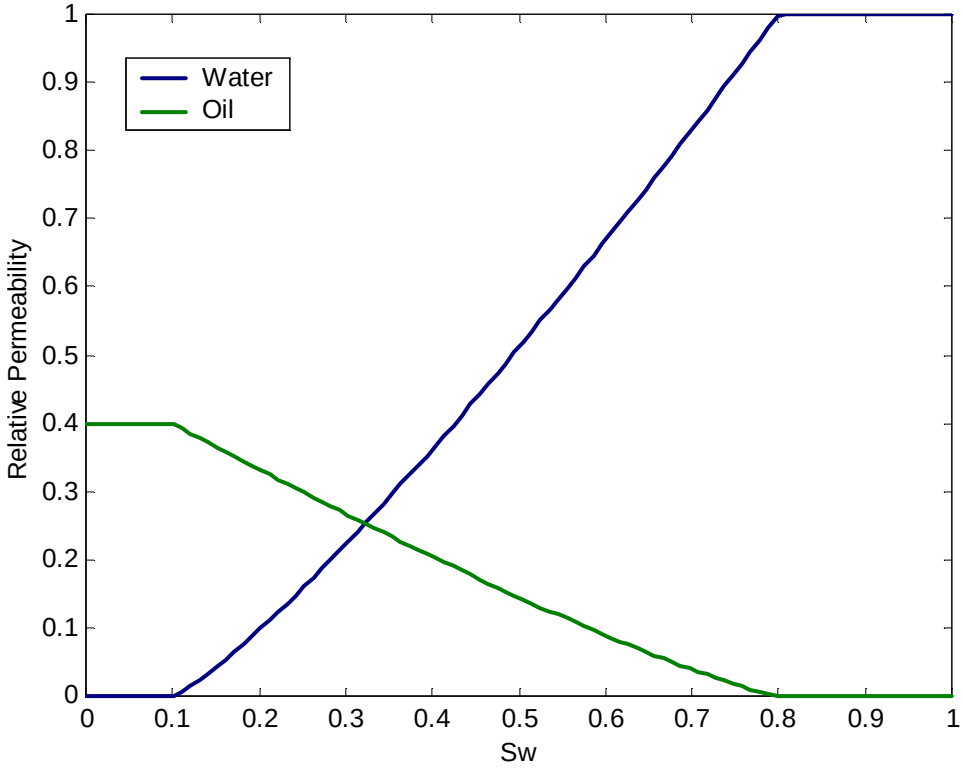

Figure (3.2): Relative permeability curves.

n_o	1.2
n_w	1.2
S_{or}	0.2
S_{wc}	0.1
k_{ro}^*	0.4
k_{rw}^*	1.0

Table (3.2): Relative permeability parameters.

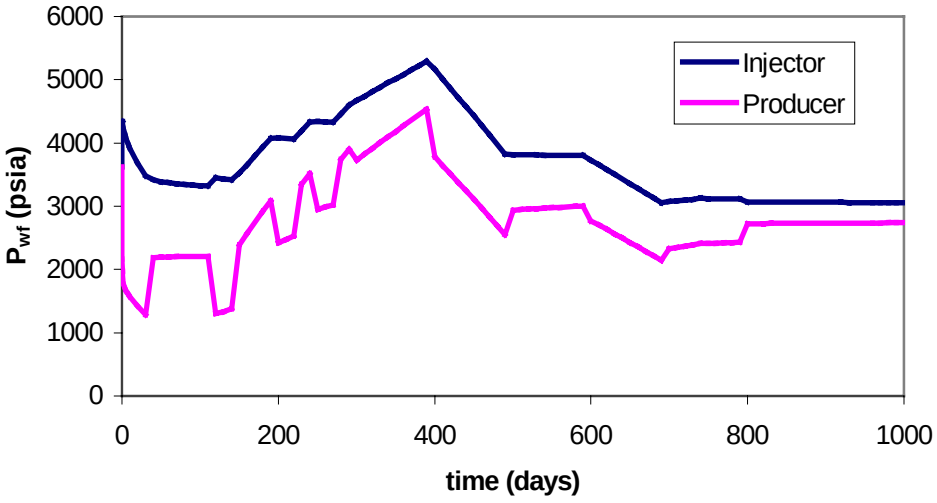

Figure (3.3): Bottom hole pressure for injector and producer wells.

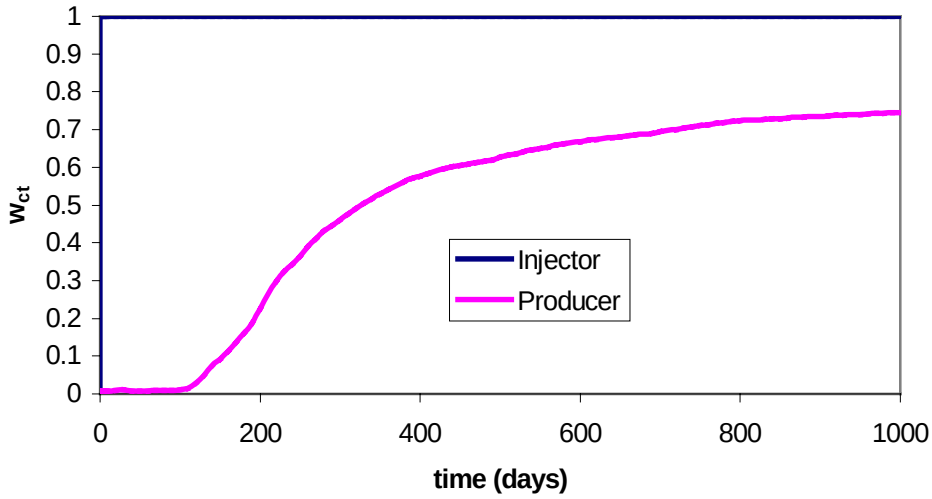

Figure (3.4): Water cut for injector and producer wells.

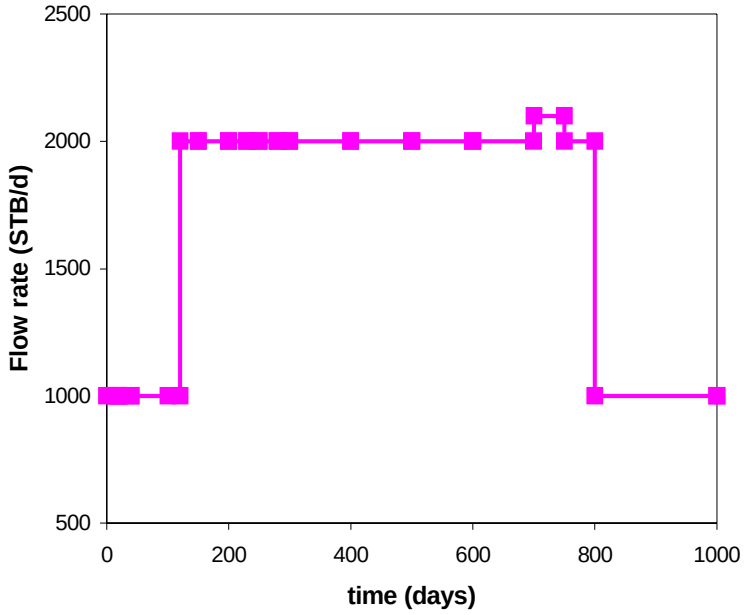

Figure (3.5): Flow rate for producer well.

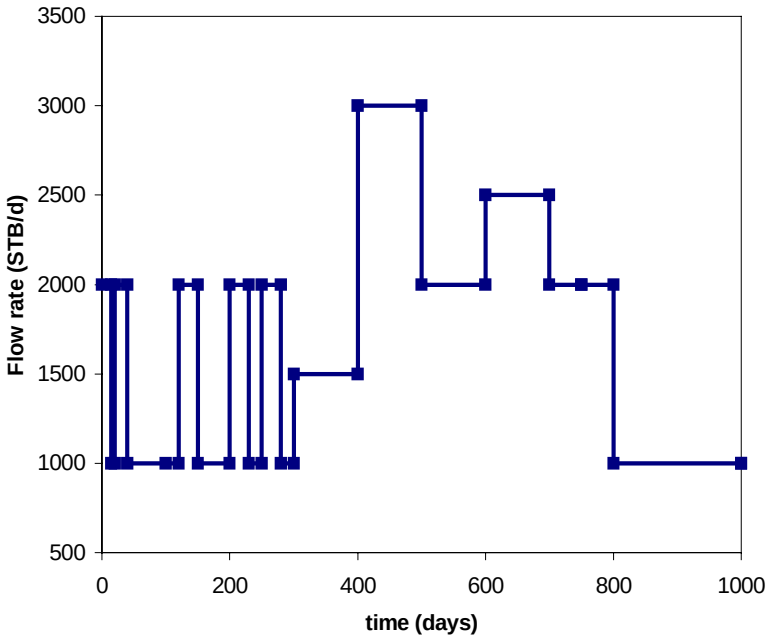

Figure (3.6): Flow rate for injector well.

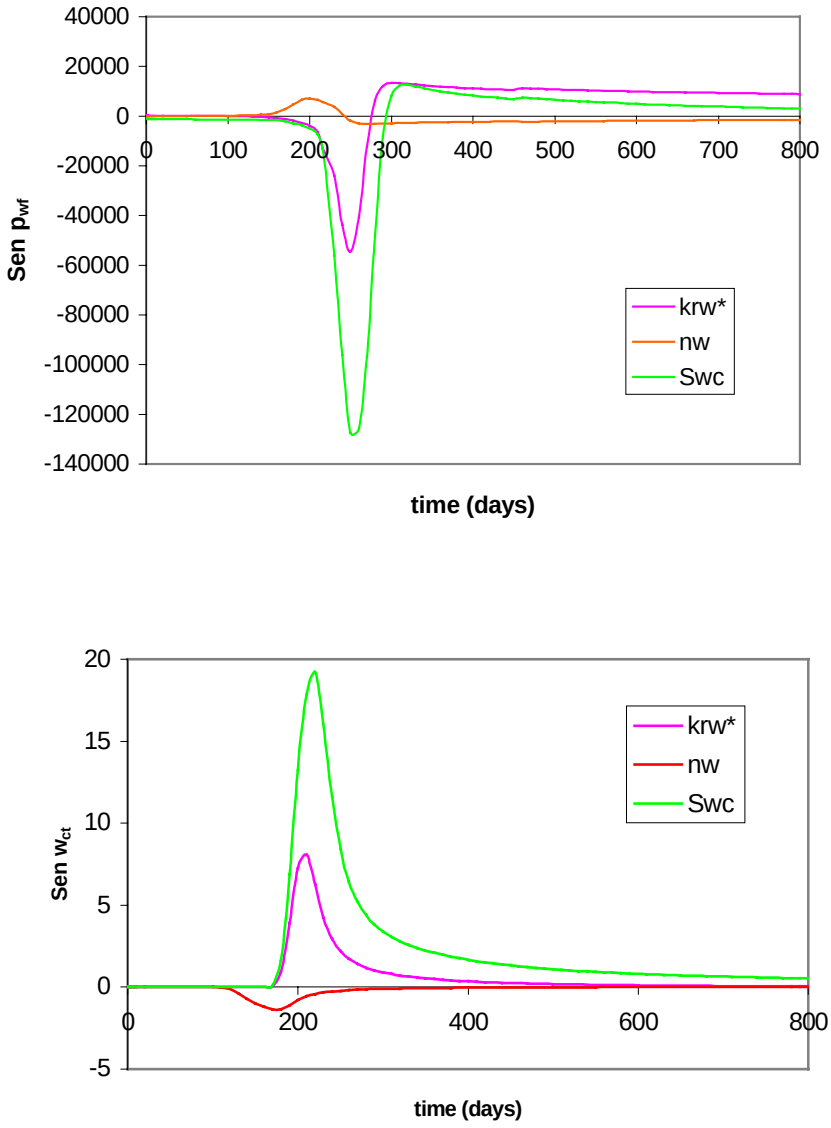

Figure (3.7): Sensitivity of pressure and water cut at producer with respect to the relative permeability parameters.

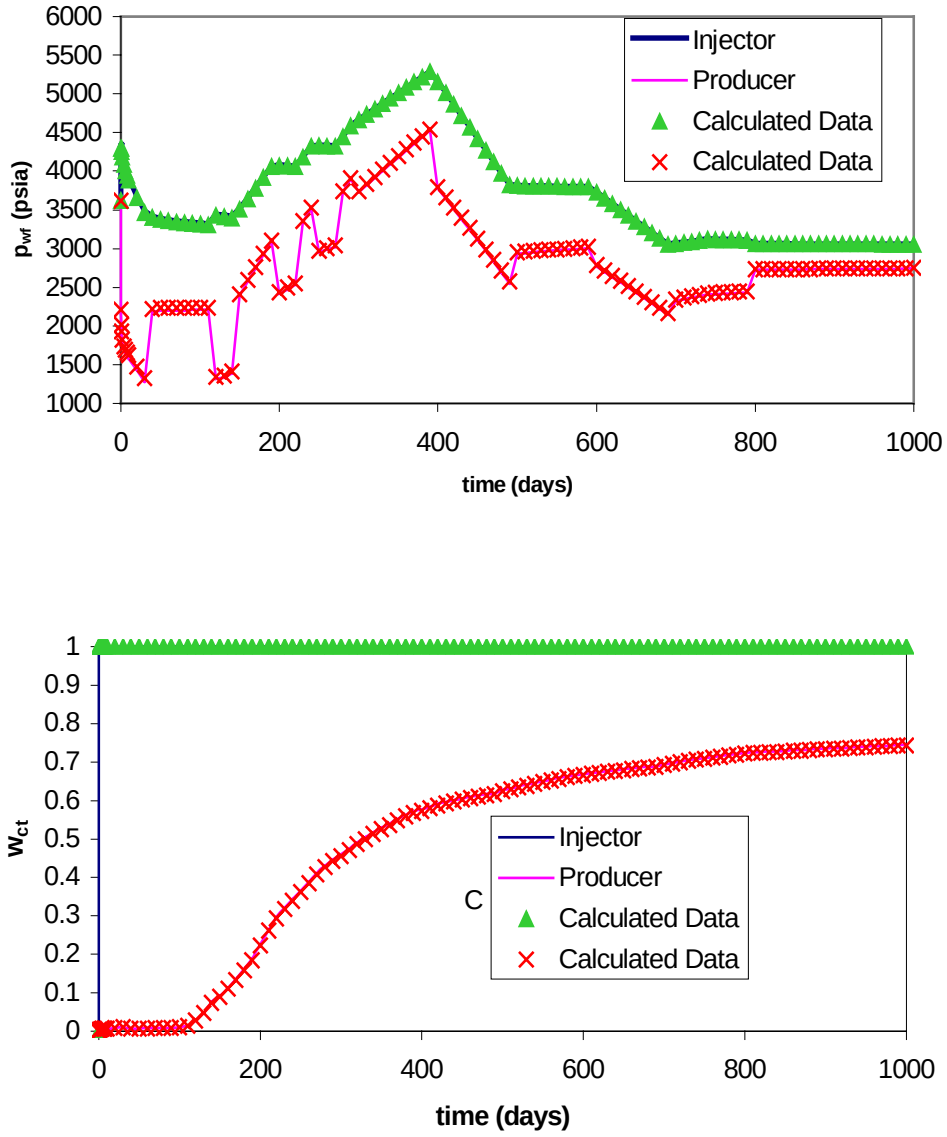

Figure (3.8): Match of bottom hole pressure and water cut for absolute permeabilities (*x*-coordinate) and the end point of the water relative permeability curve.

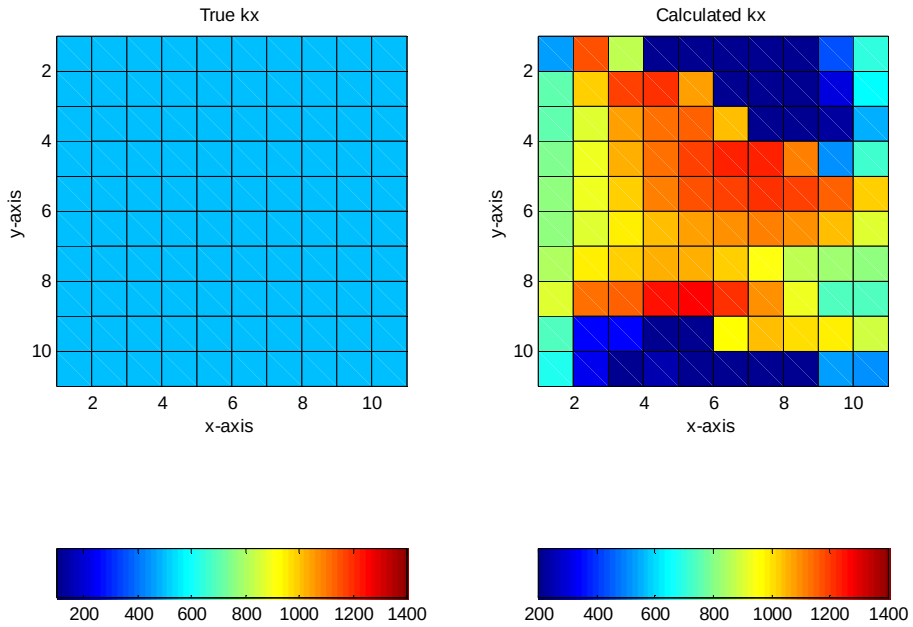

$k_{x\ initial} = 300\ md$ $\qquad$ $k_x^{avg} = 775\ md$

$k^*_{rw\ initial} = 0.8$ $\qquad$ $k^*_{rw\ final} = 1.04$

Figure (3.9): Estimated absolute permeabilities (*x*-coordinate) and the end point of the water relative permeability curve.

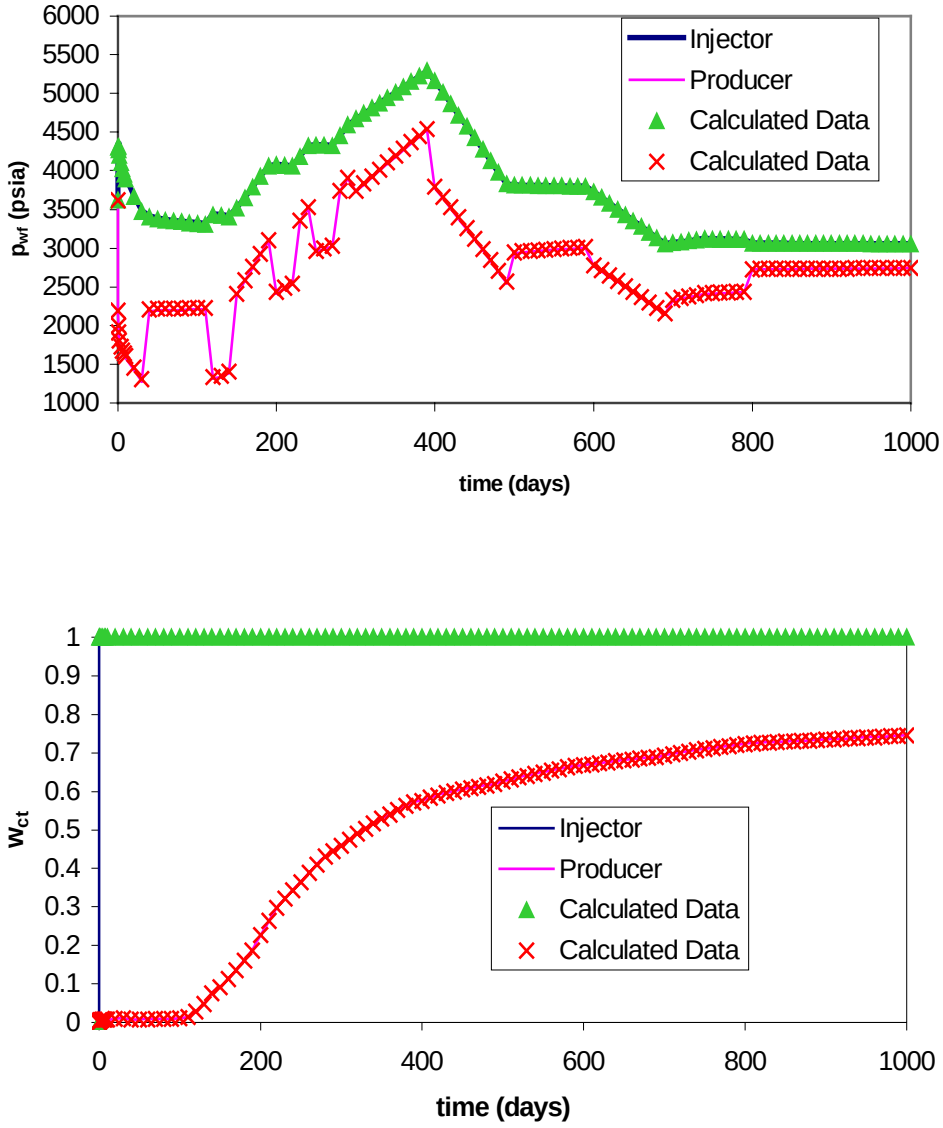

Figure (3.10): Match of bottom hole pressure and water cut for absolute permeabilities (*x*-coordinate) and the exponent of the water relative permeability curve.

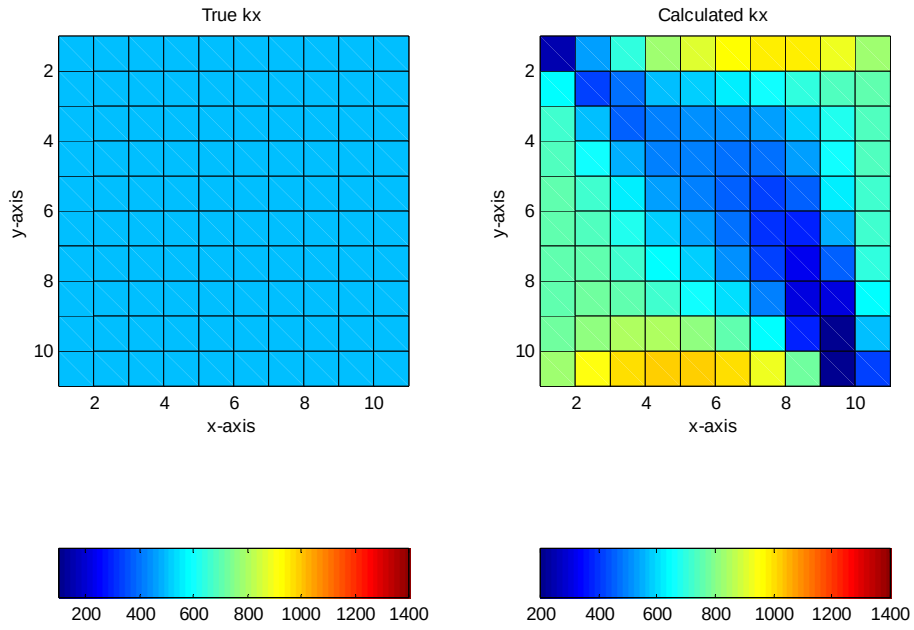

$k_{x\ initial} = 300\ md$ $k_x^{avg} = 636\ md$

$n_{w\ init} = 0.9$ $n_{w\ final} = 1.43$

Figure (3.11): Estimated absolute permeabilities (*x*-coordinate) and the exponent of the water relative permeability curve.

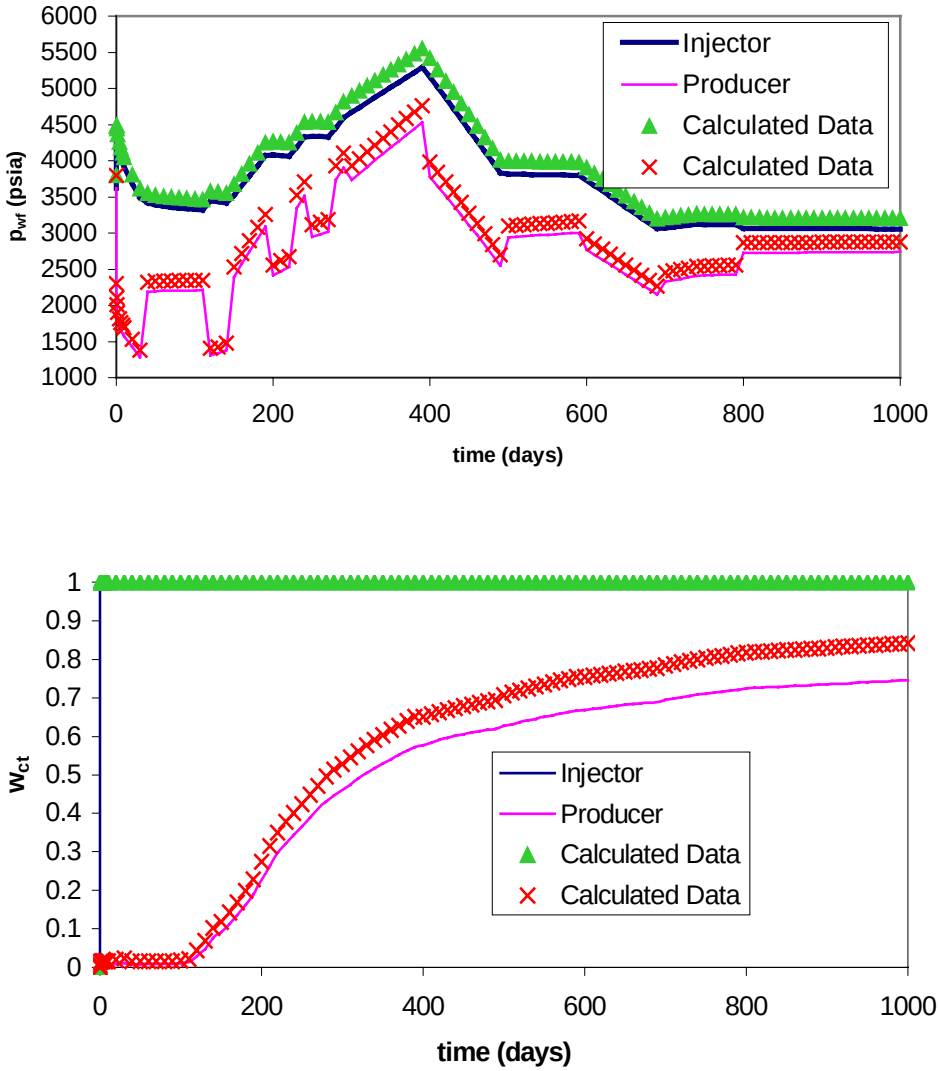

Figure (3.12): Match of bottom hole pressure and water cut for absolute permeabilities (*x*-coordinate) and connate water saturation.

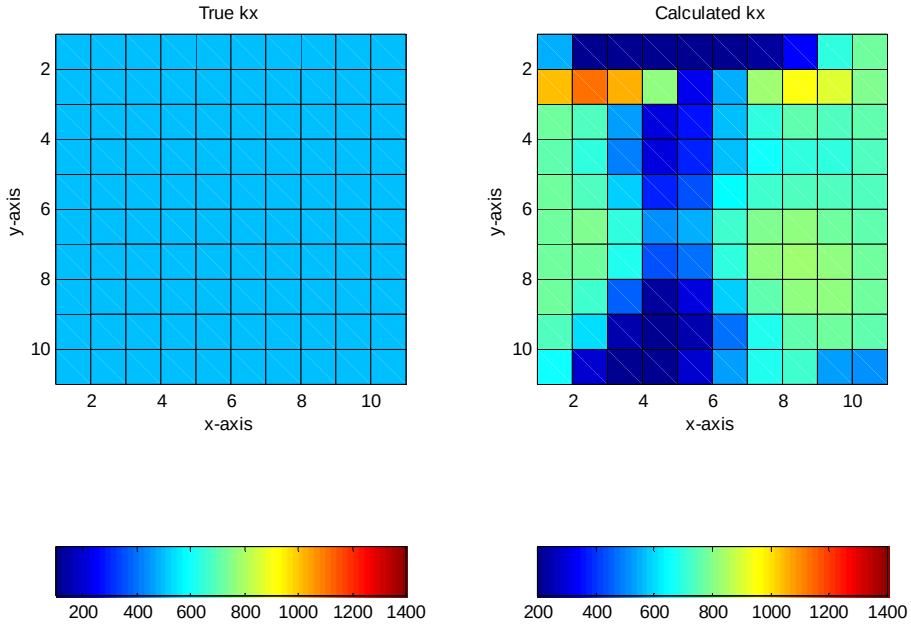

$k_{x\ initial} = 300\ md$ $k_x^{avg} = 606\ md$

$S_{wc\ initial} = 0.05$ $S_{wc\ final} = 0.11$

Figure (3.13): Estimated absolute permeabilities (*x*-coordinate) and connate water saturation.

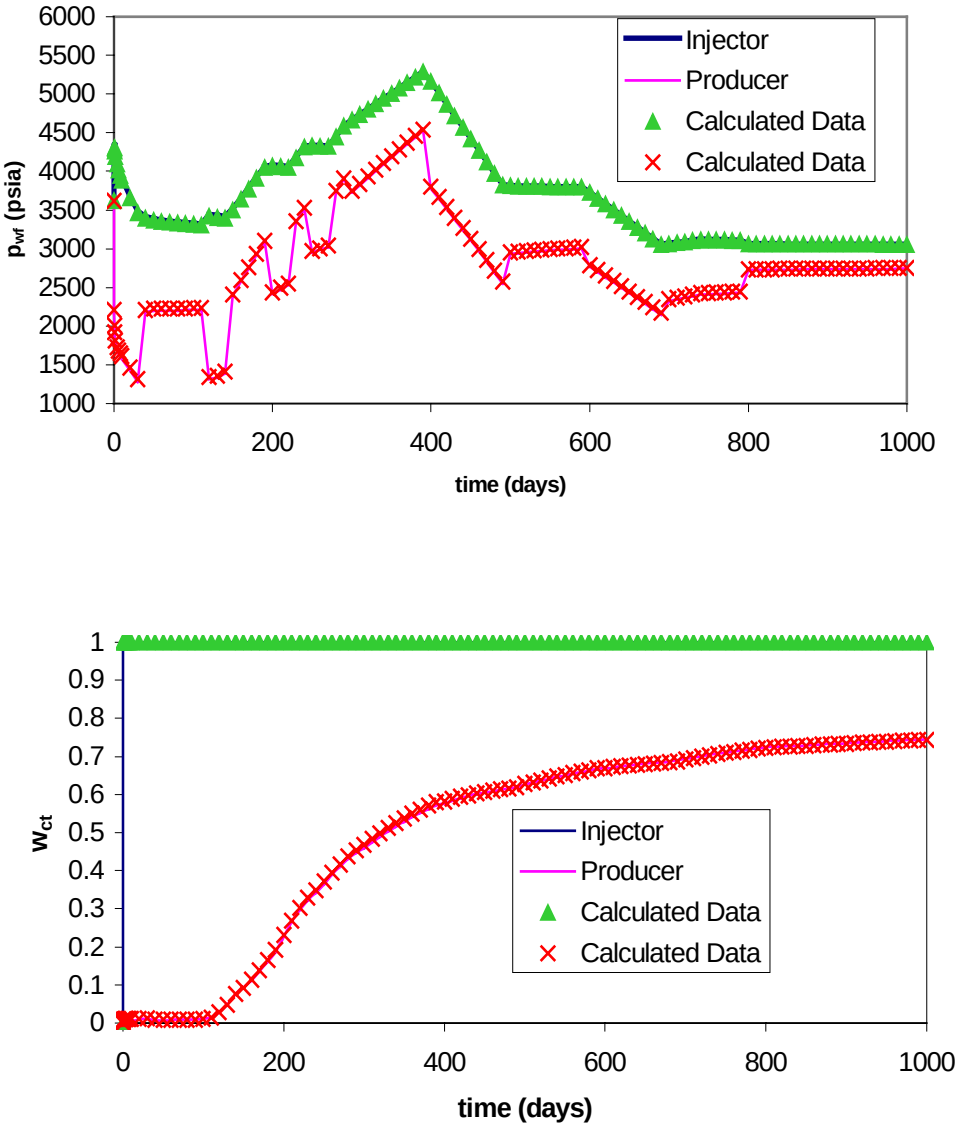

Figure (3.14): Match of bottom hole pressure and water cut for absolute permeabilities (*x*-coordinate) and the end point of the oil relative permeability curve.

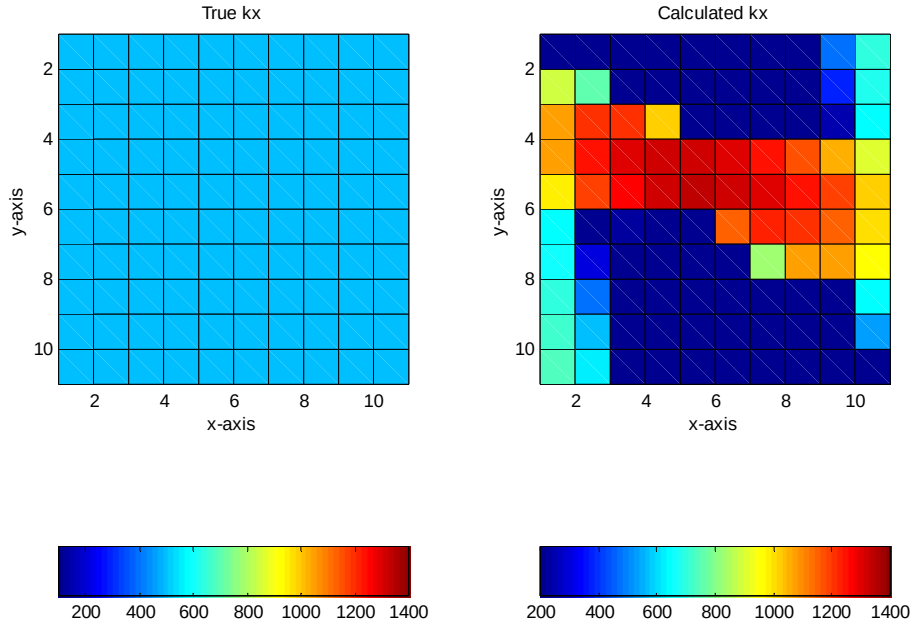

$k_{x\ initial} = 300\ md$ $\qquad$ $k_x^{avg} = 544\ md$

$k^*_{ro\ initial} = 0.80$ $\qquad$ $k^*_{ro\ final} = 0.67$

Figure (3.15): Estimated absolute permeabilities (*x*-coordinate) and the end point of the oil relative permeability curve.

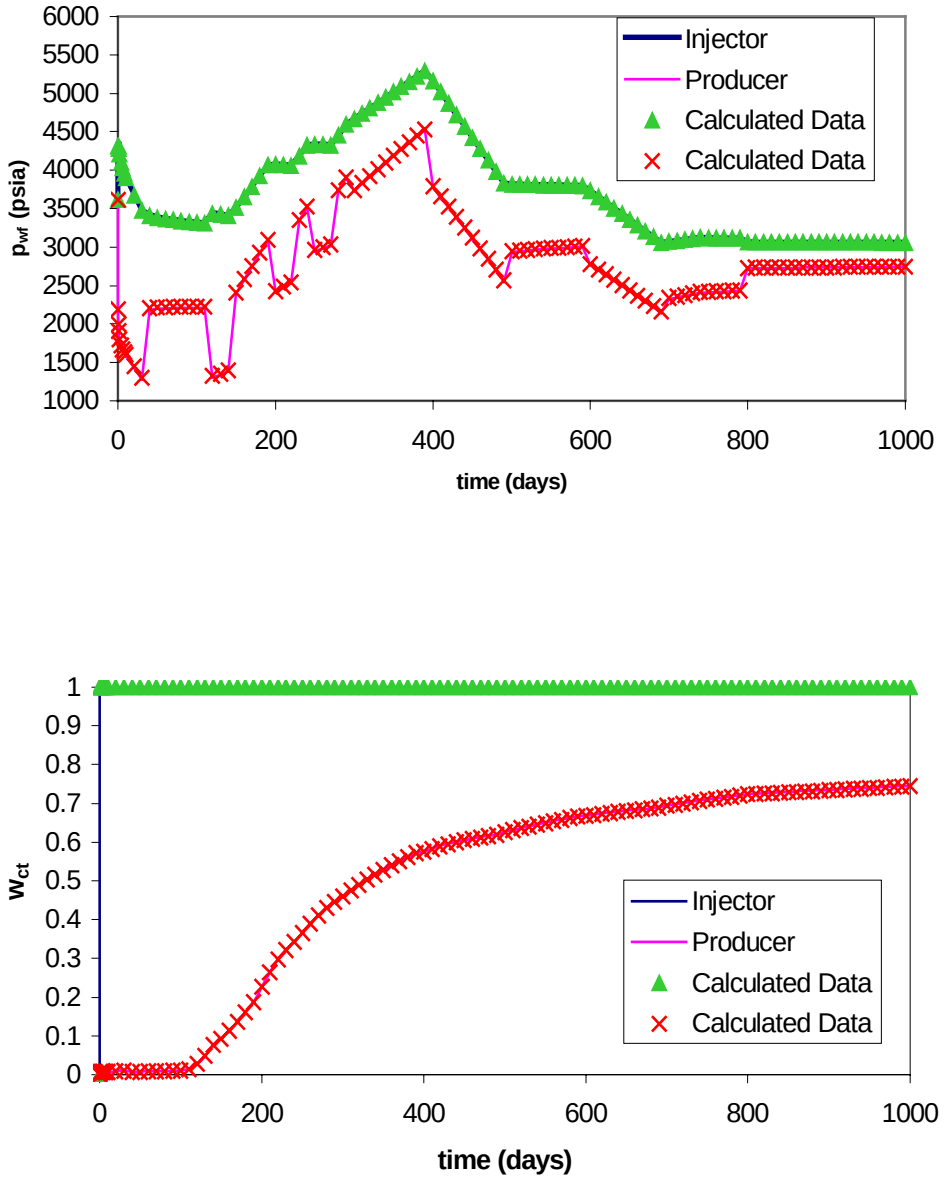

Figure (3.16): Match of bottom hole pressure and water cut for absolute permeabilities (*x*-coordinate) and the exponent of the oil relative permeability curve.

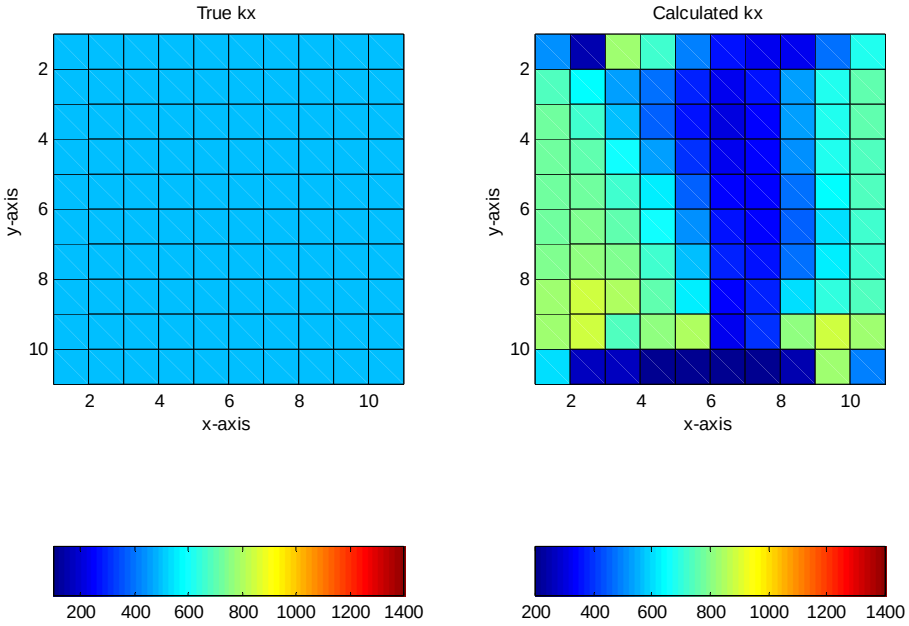

$k_{x\ initial} = 300\ md$ $k_x^{avg} = 568\ md$

$n_{o\ init} = 0.80$ $n_{o\ final} = 1.32$

Figure (3.17): Estimated absolute permeabilities (*x*-coordinate) and the exponent of the oil relative permeability curve.

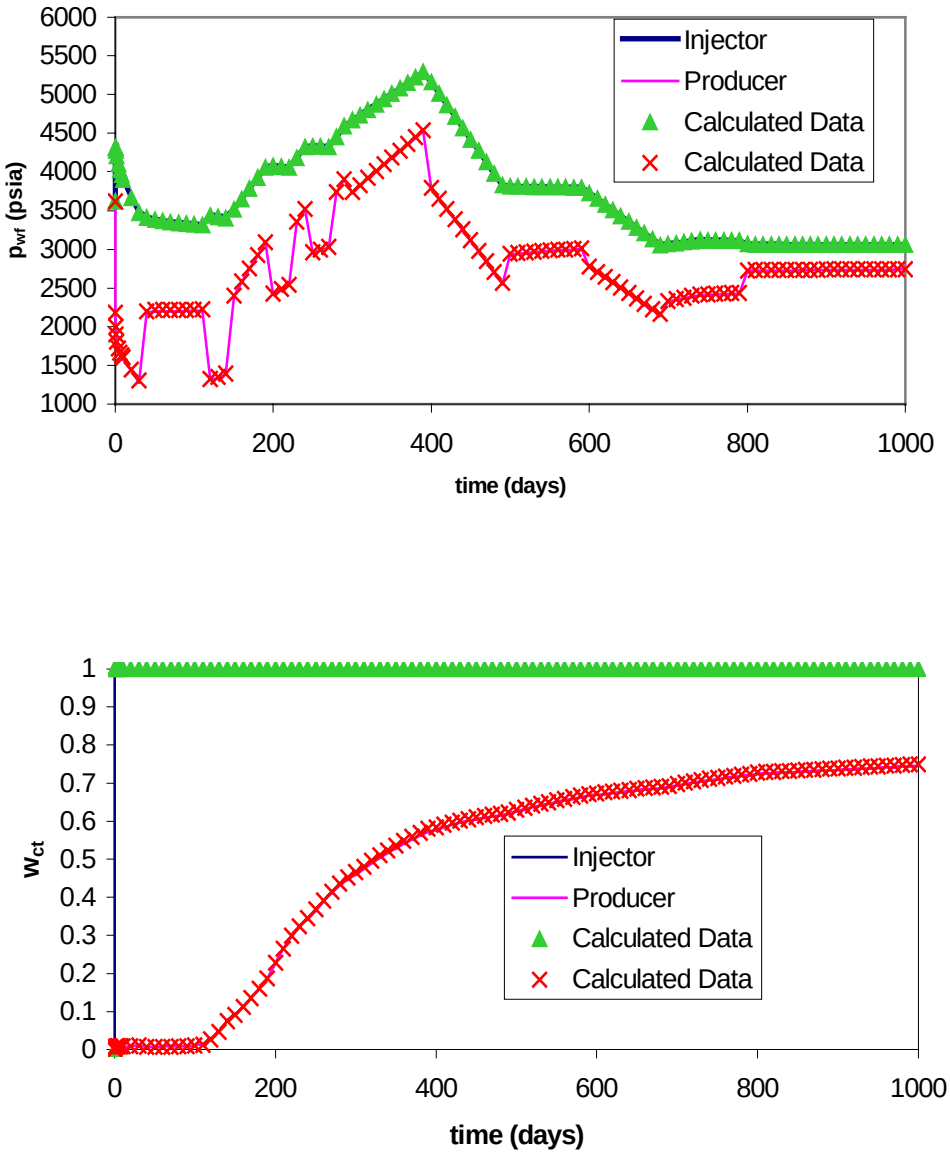

Figure (3.18): Match of bottom hole pressure and water cut for absolute permeabilities (*x*-coordinate) and residual oil saturation.

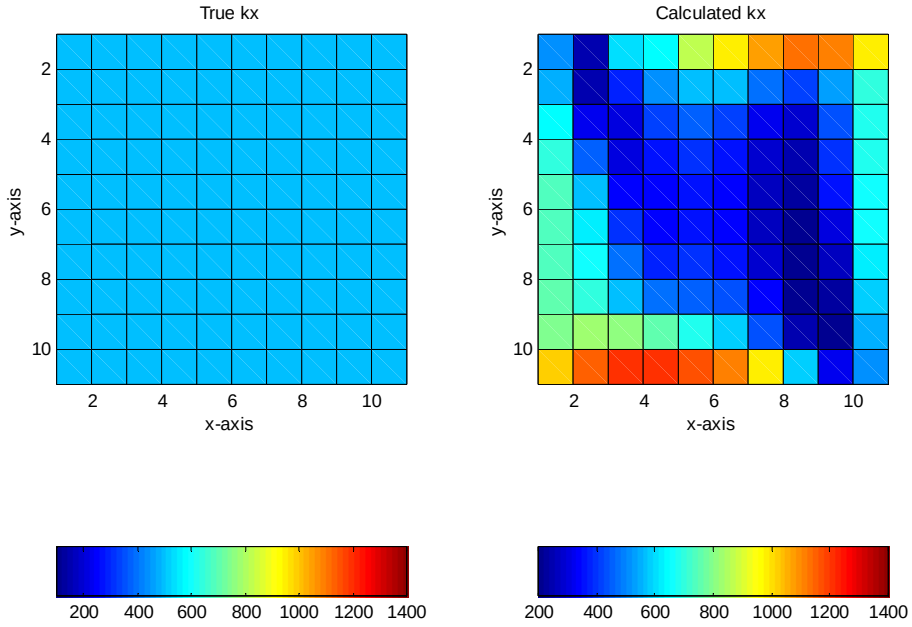

$k_{x\ initial} = 300\ md$ $k_x^{avg} = 510\ md$

$S_{or\ initial} = 0.30$ $S_{or\ final} = 0.39$

Figure (3.19): Estimated absolute permeabilities (*x*-coordinate) and oil residual saturation.

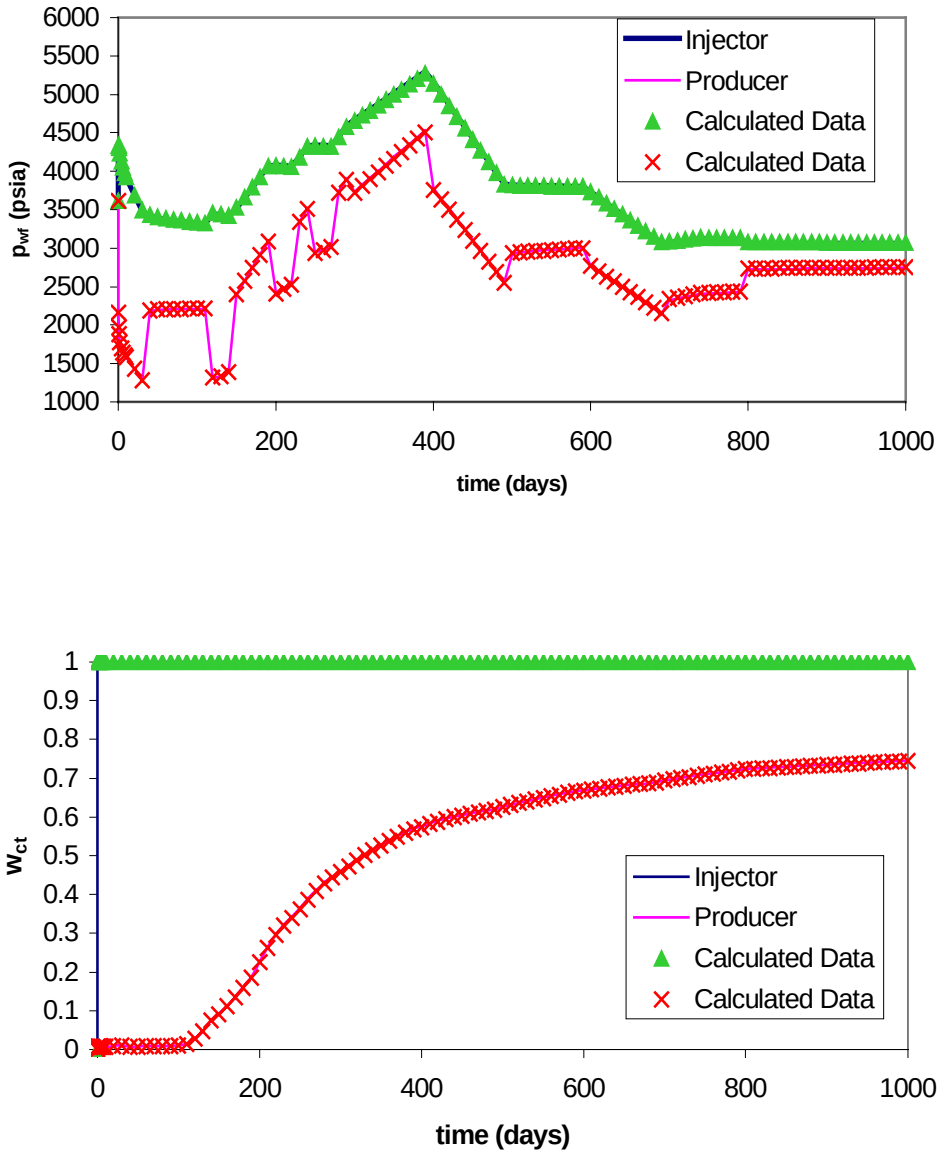

Figure (3.20): Match of bottom hole pressure and water cut for porosities and the end point of the water relative permeability curve.

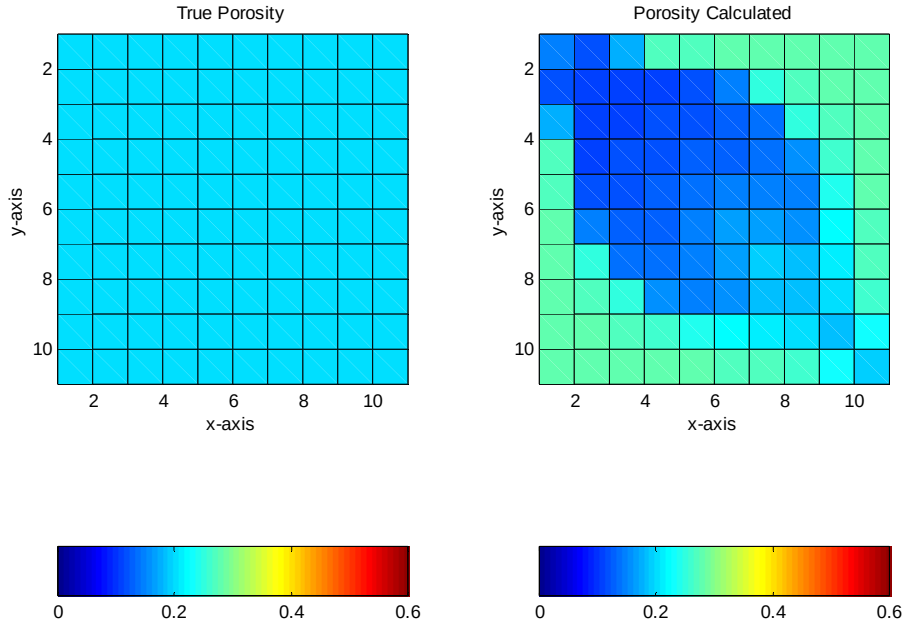

$\phi_{initial} = 0.10$ $\phi^{avg} = 0.20\ md$

$k^{*}_{rw\ initial} = 0.8$ $k^{*}_{rw\ final} = 1.03$

Figure (3.21): Estimated porosities and the end point of the water relative permeability curve.

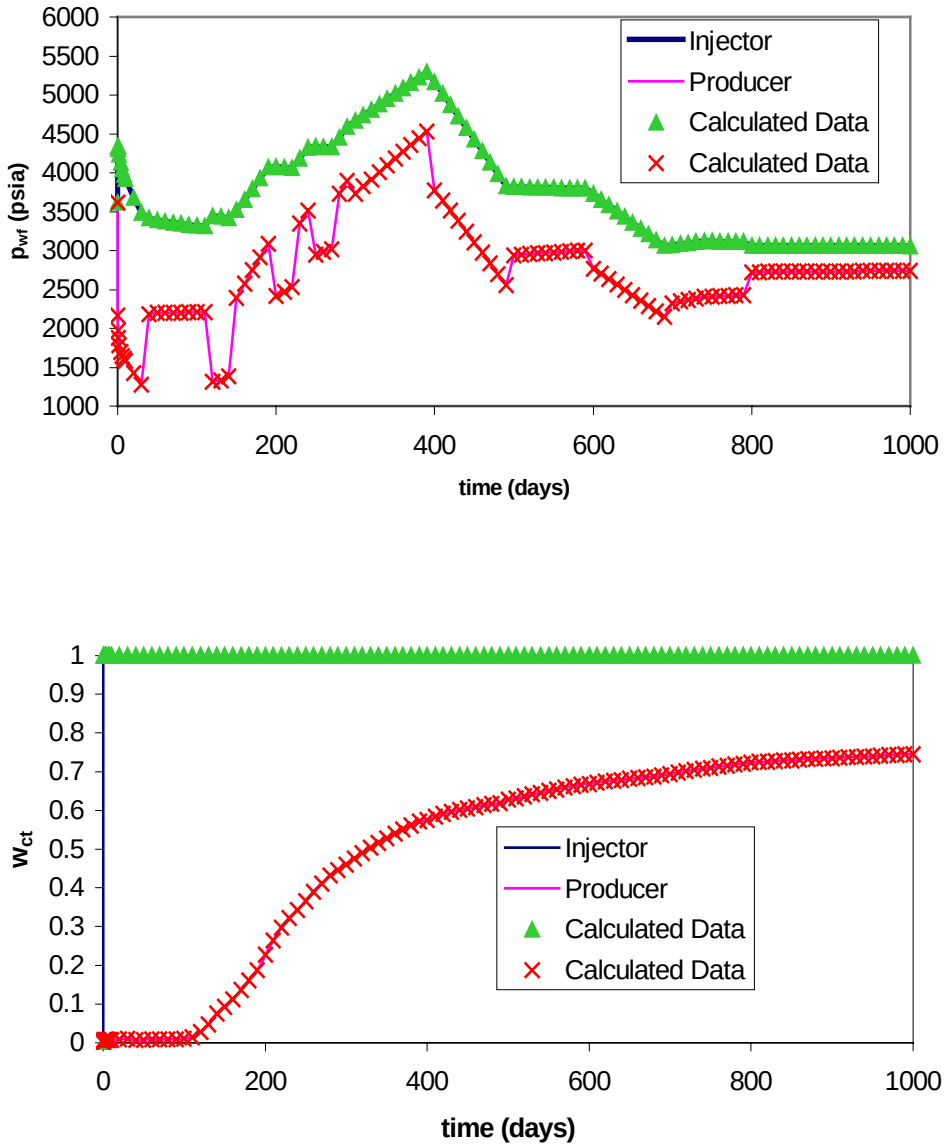

Figure (3.22): Match of bottom hole pressure and water cut for porosities (*x*-coordinate) and the exponent of the water relative permeability curve.

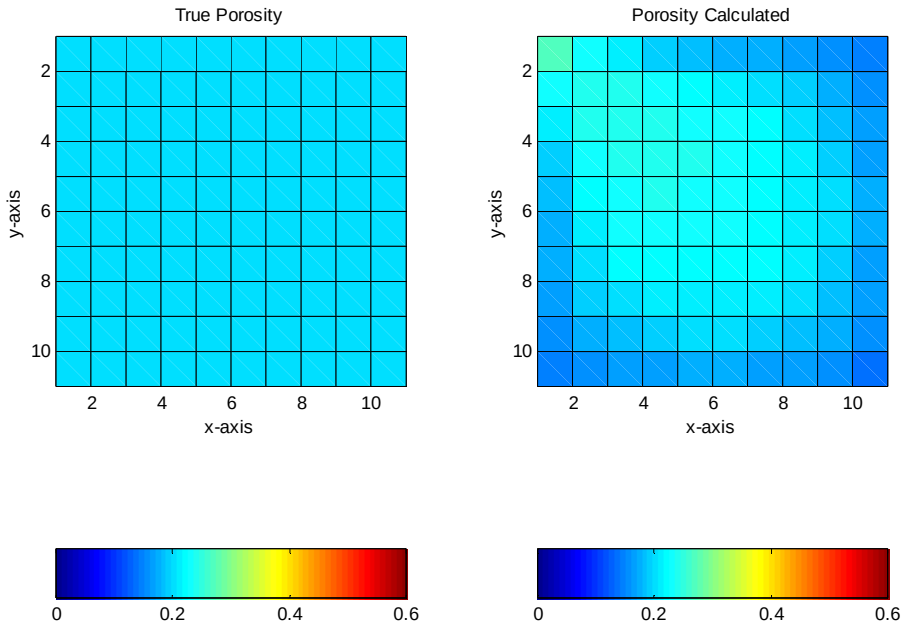

$\phi_{initial} = 0.10$ $\phi^{avg} = 0.20\ md$

$n_{w\ initial} = 0.90$ $n_{w\ final} = 0.98$

Figure (3.23): Estimated porosities and the exponent of the water relative permeability curve.

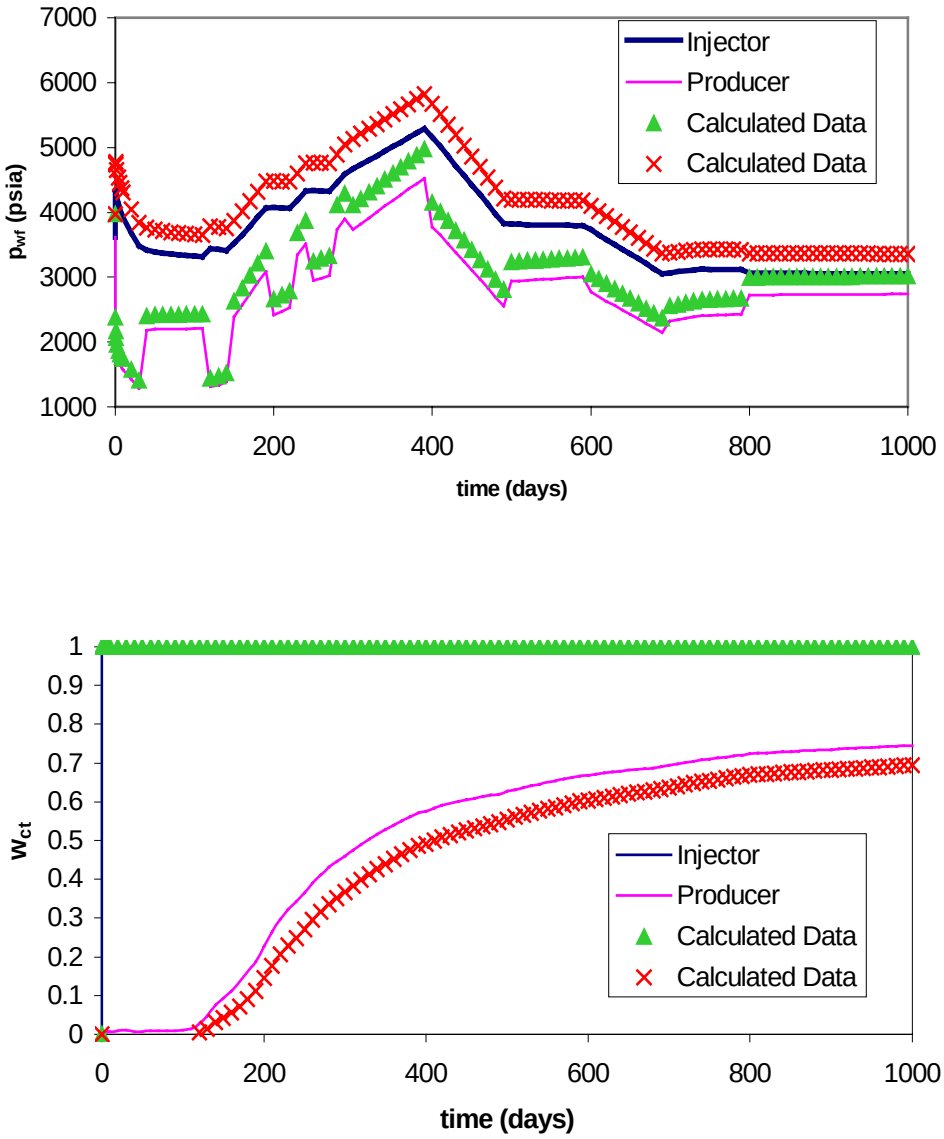

Figure (3.24): Match of bottom hole pressure and water cut for porosities and connate water saturation.

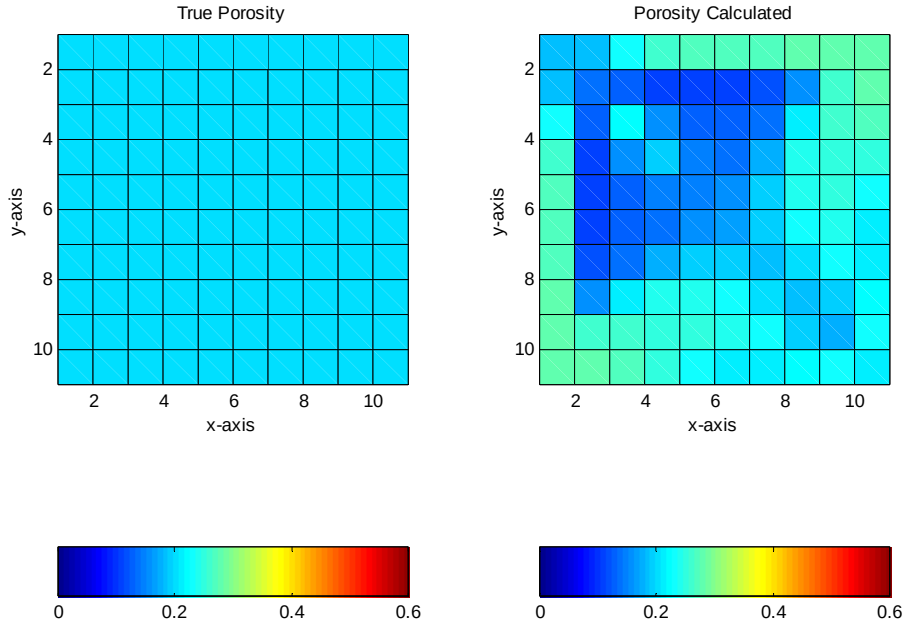

$\phi_{initial} = 0.10$ $\phi^{avg} = 0.22\ md$

$S_{wc\ initial} = 0.05$ $S_{wc\ final} = 0.10$

Figure (3.25): Estimated porosities and connate water saturation.

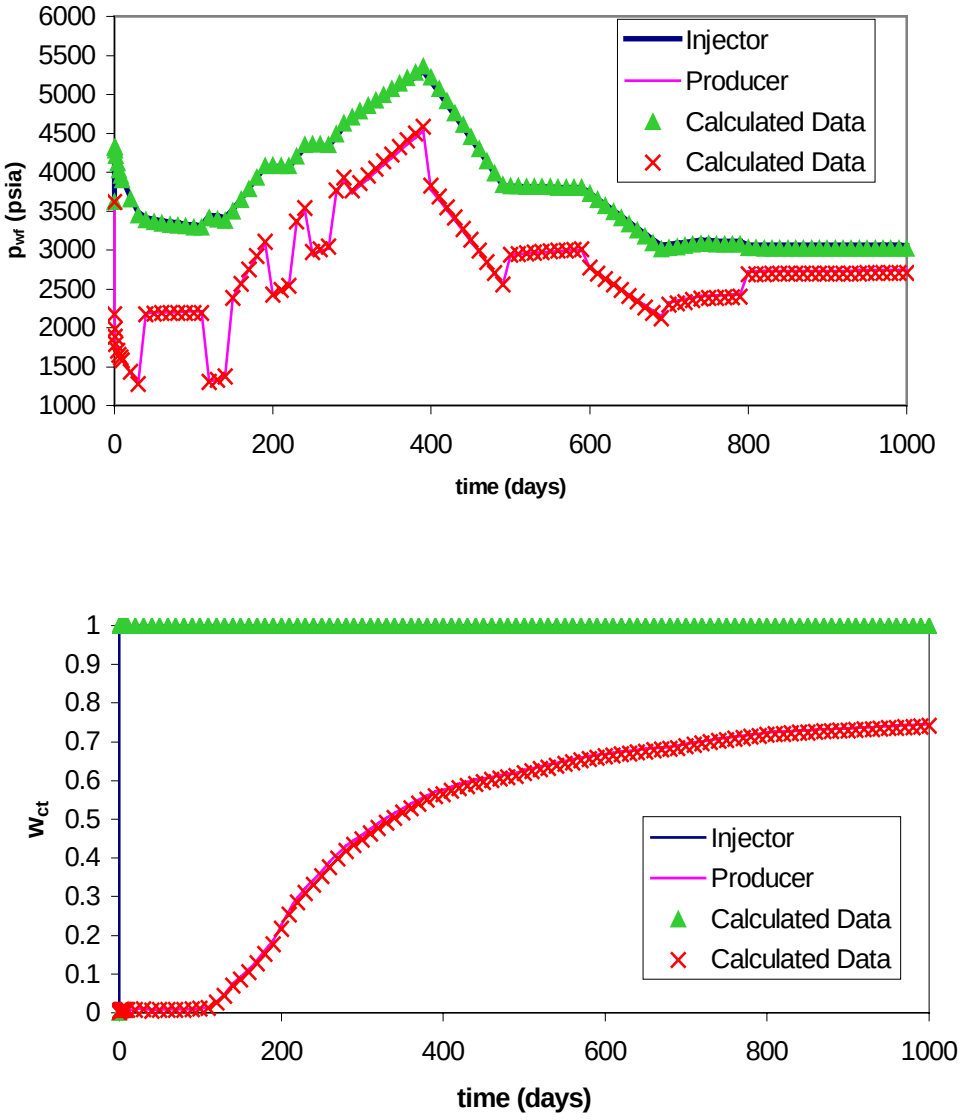

Figure (3.26): Match of bottom hole pressure and water cut for porosities and the end point of the oil relative permeability curve.

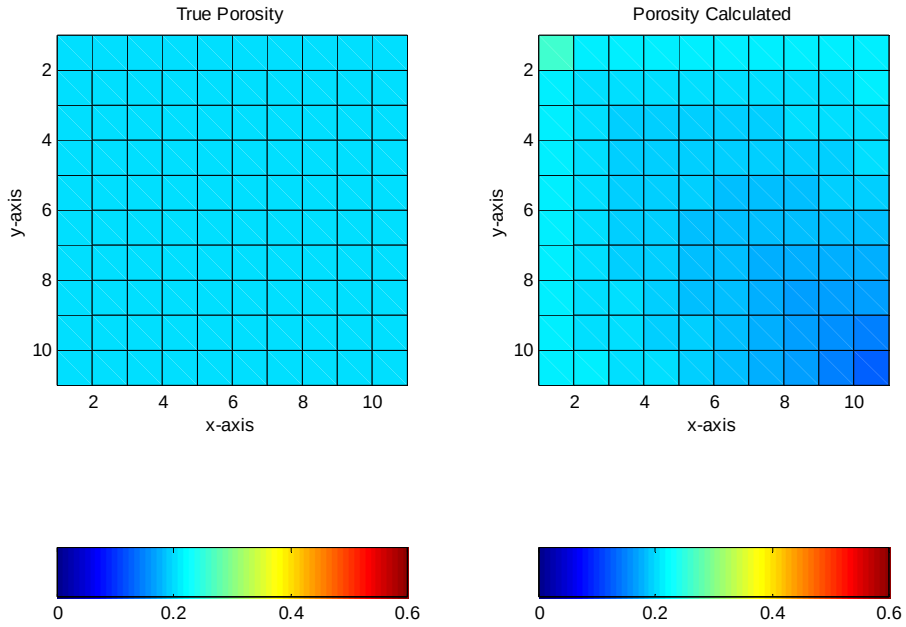

$\phi_{initial} = 0.10$ $\phi^{avg} = 0.19\ md$

$k^{*}_{ro\ initial} = 0.80$ $k^{*}_{ro\ final} = 0.34$

Figure (3.27): Estimated porosities and the end point of the oil relative permeability curve.

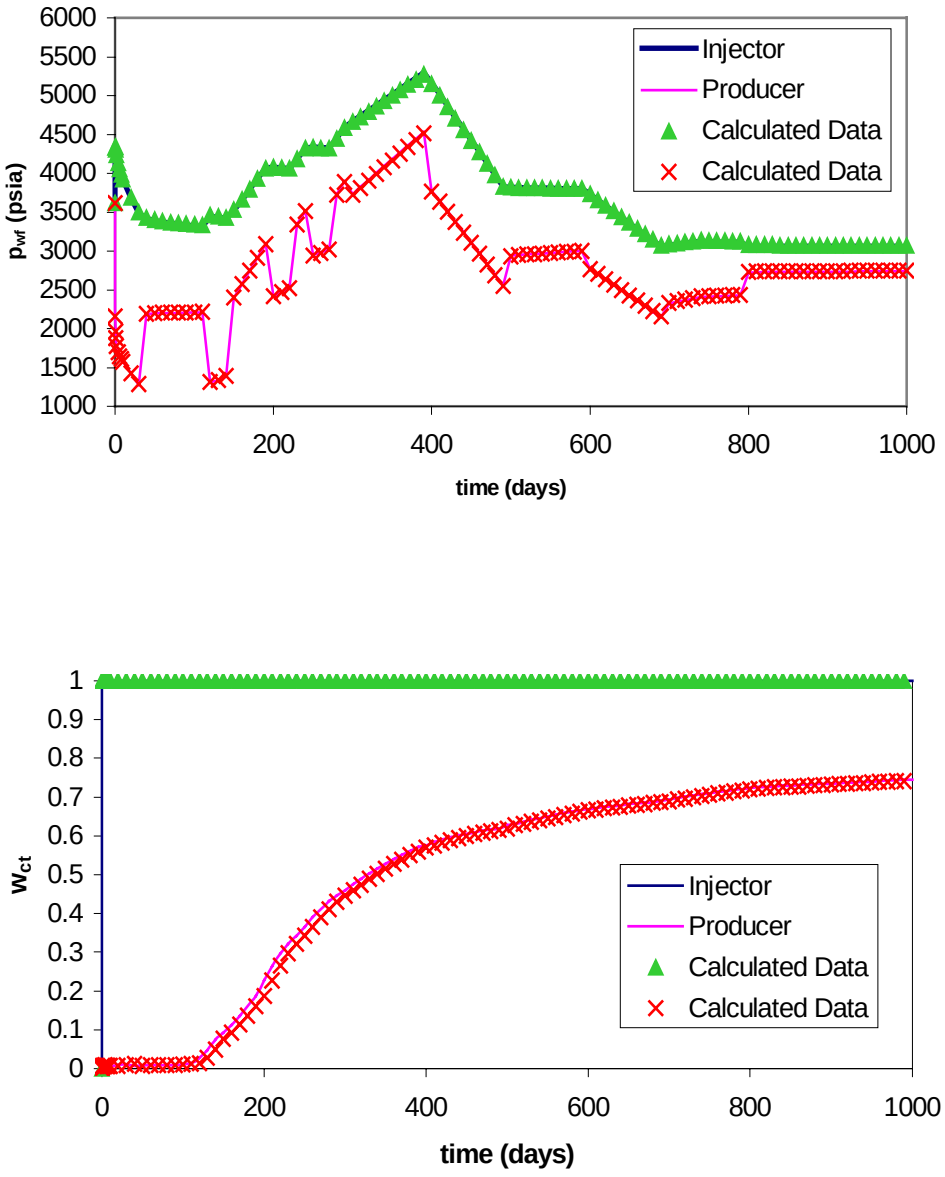

Figure (3.28): Match of bottom hole pressure and water cut porosities and the exponent of the oil relative permeability curve.

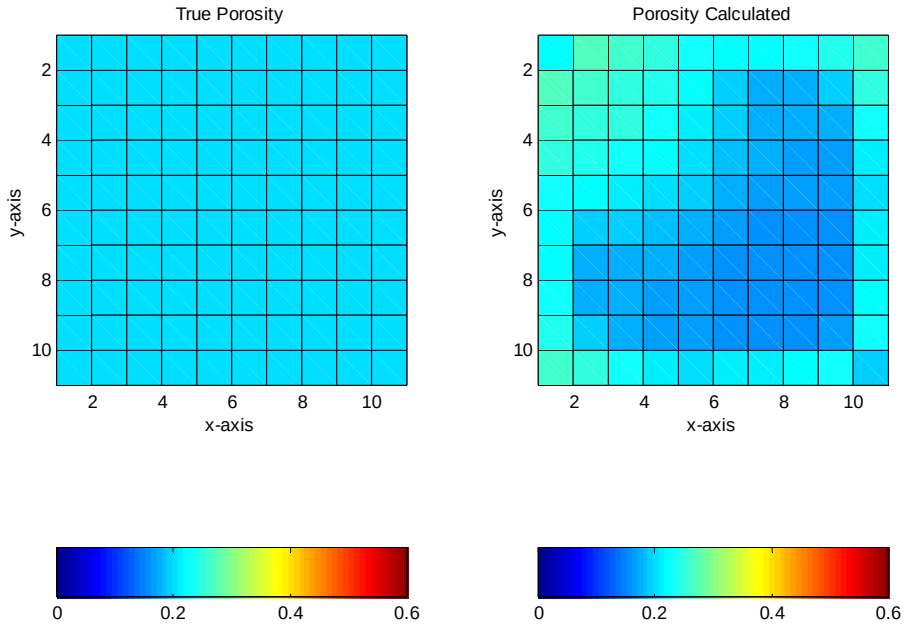

$\phi_{initial} = 0.10$ $\phi^{avg} = 0.20\ md$

$n_{o\ initial} = 0.80$ $n_{o\ final} = 1.36$

Figure (3.29): Estimated porosities and the exponent of the oil relative permeability curve.

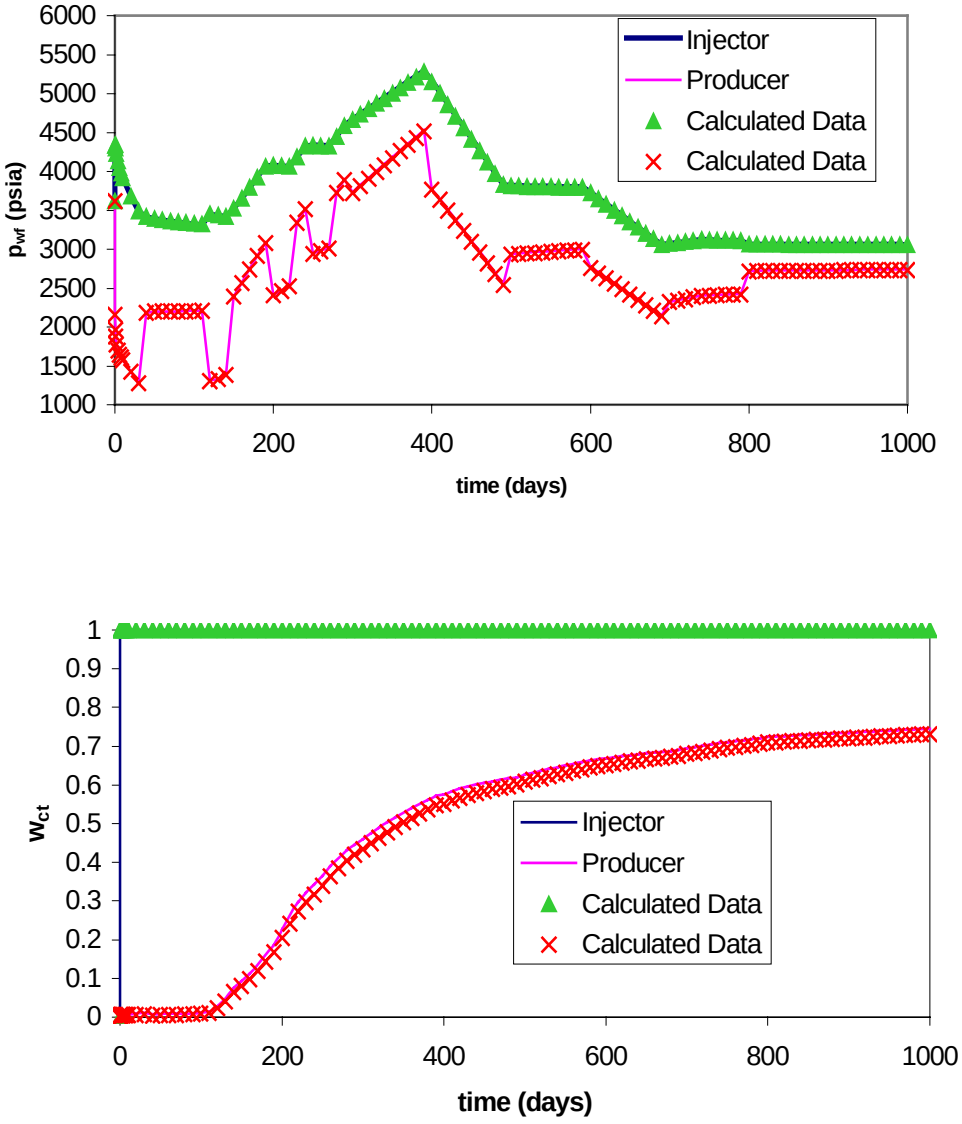

Figure (3.30): Match of bottom hole pressure and water cut for porosities and residual oil saturation.

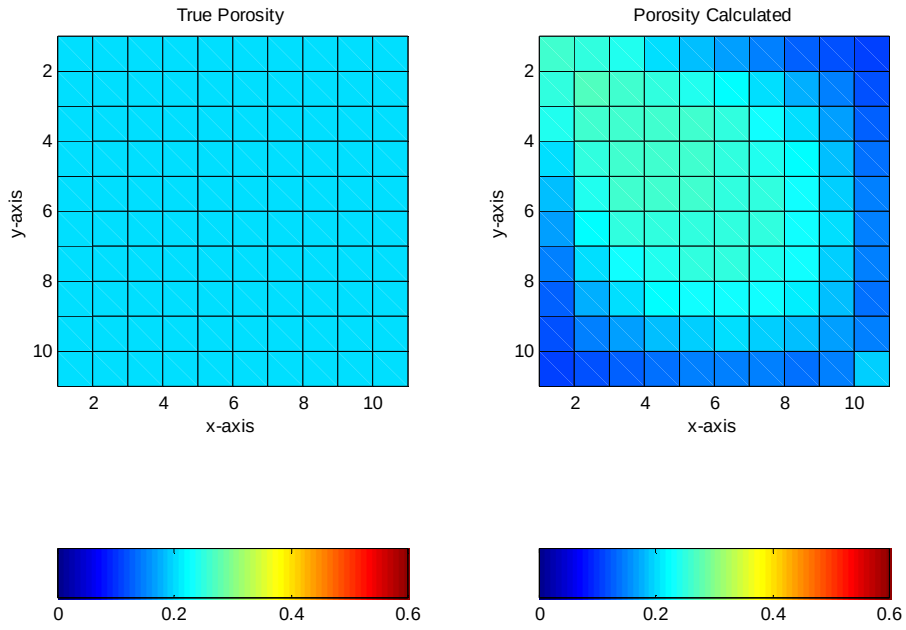

$\phi_{initial} = 0.10$ $\phi^{avg} = 0.20\ md$

$S_{or\ initial} = 0.30$ $S_{or\ final} = 0.33$

Figure (3.31): Estimated porosities and oil residual saturation.

Section 4

Conclusions and Recommendations

This work discussed the influence of the relative permeability in the inverse problem to estimate distributed parameters. The approach followed was to parameterize the relative permeabilities using the Corey model and then treat those parameters as unknowns along with absolute permeabilities and porosities. Based on the results of the test cases discussed in the previous section, the following conclusions can be drawn.

- Sensitivity coefficients, as measures of the information about the parameters being estimated, indicate the importance of recording data when the breakthrough occurs as well as the relationship between the parameters.

- The absolute permeability distribution is much more sensitive to the relative permeabilities than porosity distribution. Indeed, using wrong relative permeabilities may not affect the porosity distribution to a great extent.

- Connate water saturations and residual oil saturations should be obtained using others sources instead of including them in the data inversion problem because the

high degree of uncertainty they may add to the parameter estimation. Besides, including them in the inversion increases the computer cost.

- In order to avoid the inverse model converging to a channel pattern model, geological information should be integrated in the inverse model.

- External sources of information such as rock wettabilities or residual saturations should be included to constrain relative permeability if they are included in the invese problem.

- As was stated in Section 2, the numerical model used in this work does not include capillary forces. Since relative permeabilities have a strong dependence on them, capillary pressure should be considered in the model in future works.

Nomenclature

B	Formation volume factor
c	Compressibility
d	data
g	Gravity constant
$\underline{\underline{G}}$	Sensitivity matrix
$\underline{\underline{H}}$	Hessian matrix
$\underline{\underline{H}}_{GN}$	Gauss-Newton Hessian matrix approximation
E	Objective function
k	Absolute permeability
k_r	Relative permeability
k_{rp}^*	End point of Corey type curves ($p = o, w$)
n_p	Exponent of Corey type curves($p = o, w$)
$\vec{n}$	Normal vector to the surface
$nobs$	Number of observation
$npar$	Number of parameters
p	Pressure
q	Production or injection rate
$R_{c,p}$	Solubility of component c in phase p
S	Saturation
S_{or}	Oil residual saturation

NOMENCLATURE

S_{wc}	Connate water saturation
T	Transpose
t	time
V	Volume
$\vec{u}$	Darcy velocity vector
$\vec{x}$	Spatial coordinate vector *(x,y,z)*
w	*W*eight
$\underline{\underline{W}}$	Weight Matrix
z	Vertical direction
w_{ct}	Watercut

Symbols

α	Parameter
δ	Step size
ε	Samall number
ϕ	Porosity
λ	mobility
μ	Viscosity
ρ	Density
Δ	Difference
∇	Gradient
$\rightarrow$	Vector
$\underline{\underline{\ }}$	Matrix

NOMENCLATURE

Superscripts

0	Reference conditions
cal	Calculated data
obs	Observed data

Subscripts

c	*Component*
np	Number of phases
o	Oil phase
p	Phase
R	*Rock*
w	Water phase

Bibliography

[1] Al-Labban, Z. S.: Automatic History Matching of Relative Permeabilities Using Linear Modeling Techniques, M.S. Report, Stanford University, California (March 1990).

[2] Aziz, K: *Fundamentals of Reservoir Simulation*, Stanford University Publishers, Palo Alto, California (2001).

[3] Aziz, K. and Settari, A.: *Petroleum Reservoir Simulation*, Elsevier Applied Science Publishers, New York, New York (1979).

[4] Barua, J., Horne, R. N., Greenstadj, J. L. and Lopez, L.: "Improved Estimation Algorithms for Automated Type Curve Analysis of Well Tests," SPE 14255 (corrected) presented at the 1985 SPE Annual Technical Conference and Exhibition, Las Vegas, Nevada, (September 22-25).

[5] Bear, J.: *Dynamics of Fluids in Porous Media*, Dover Publications Inc., Minneola, New York (1988).

[6] Chong, E. K. P. and Zak H. S.: *An Introduction to Optimization*, John Wiley & Sons, New York, New York (1996).

[7] Coats, K. H., Dernpsey, J. K., and Henderson, J. H.: "A New Technique for Determining Reservoir Description From Field Performance Data," *SPEJ* (March, 1970), 66-74.

BIBLIOGRAPHY

[8] Corey, A. T.: "The Interrelation Between Gas and Oil Relative Permeabilities," *Prod. Monthly* (Nov., 1954), 38-41.

[9] Eterkin, T., Abou-Kassem, J. H. and King, G. R.: *Basic Applied Reservoir Simulation*, SPE Textbook series vol. 7, SPE Inc. Richardson, Texas (2001).

[10] Gill, P. E., Murray, W., and Wright, M. H.: *Practical Optimization*, Academic Press, San Diego, California (1981).

[11] Horne, R. N.: *Modern Well Test Analysis: A Computer Aided Approach*, 2nd Edition, Petroway, Palo Alto, California (1995).

[12] Jones, S. C., and Roszelle, W. O.: "Graphical Techniques for Determining Relative Permeability From Displacement Experiments," *JPT* (May, 1978), 807-817.

[13] Landa, J. L., Kamal, M. M., Jenkins, C. D., and Horne, R. N.: "Reservoir Characterization Constrained to Well Test Data: A Field Example," SPE 36511 presented at the 1996 SPE Annual Technical Conference and Exhibition, Denver, Colorado, (October, 6-9).

[14] Landa, J. L.: Reservoir Parameter Estimation Constrained to Pressure Transients, Performance History and Distributed Saturation Data, PhD dissertation, Stanford University, California (June 1997).

[15] Landa, J. L.: "Technique to Integrate Production and Static Data in Self-Consistent WAY," SPE 71597 presented at the 2001 SPE Annual Technical Conference and Exhibition, New Orleans, Louisiana, (September 30 – October 3)

[16] Mamora, D. D.: Automatic History Matching to Determine Relative Permeabilities, M.S. Report, Stanford University, California (February 1990).

[17] Peaceman, D. W.: *Fundamentals of Numerical Reservoir Simulation*, Elsevier Scientific Publications, New York, New York (1977).

[18] Phan, V. Q.: Inferring Depth-Dependent Reservoir Properties from Integrated Analysis Using Dynamic Data, M.S. Report, Stanford University, California (June1998).

[19] Phan, V. Q. and Horne, R. N.: "Determining Depth-Dependent Reservoir Properties Using Integrated data Analysis," SPE 56423 presented at the 1999 SPE Annual Technical Conference and Exhibition, Houston, Texas, (October 3-6)

[20] Press, W. H., Teukolsky, S. A., Vetterling, W. T., and Flannery, B. P.: *Numerical Recipes in Fortran 77: The Art of Scientic Computing*, vol. 1, Second Edition, Cambridge University Press, New York, New York (1996).

[21] Rosa, A. J.: Automated Type Curve Matching in Well Test Analysis, M.S. Report, Stanford University, California (March 1983).